International Ocean Discovery Program
Expedition 396 Scientific Prospectus

Mid-Norwegian Continental Margin Magmatism

Sverre Planke
Co-Chief Scientist
Department of Geosciences
University of Oslo
and
Volcanic Basin Petroleum Research AS
Norway

Christian Berndt
Co-Chief Scientist
Department of Marine Geodynamics
GEOMAR Helmholtz Centre for Ocean Research Kiel
Germany

Carlos A. Alvarez Zarikian
Expedition Project Manager/Staff Scientist
International Ocean Discovery Program
Texas A&M University
USA

IODP
INTERNATIONAL OCEAN
DISCOVERY PROGRAM

Publisher's notes

This publication was prepared by the *JOIDES Resolution* Science Operator (JRSO) at Texas A&M University (TAMU) as an account of work performed under the International Ocean Discovery Program (IODP). This material is based upon work supported by the JRSO, which is a major facility funded by the National Science Foundation Cooperative Agreement Number OCE1326927. Funding for IODP is provided by the following international partners:

National Science Foundation (NSF), United States
Ministry of Education, Culture, Sports, Science and Technology (MEXT), Japan
European Consortium for Ocean Research Drilling (ECORD)
Ministry of Science and Technology (MOST), People's Republic of China
Korea Institute of Geoscience and Mineral Resources (KIGAM)
Australia-New Zealand IODP Consortium (ANZIC)
Ministry of Earth Sciences (MoES), India
Coordination for Improvement of Higher Education Personnel (CAPES), Brazil

Portions of this work may have been published in whole or in part in other IODP documents or publications.

This IODP *Scientific Prospectus* is based on precruise *JOIDES Resolution* Facility advisory panel discussions and scientific input from the designated Co-Chief Scientists on behalf of the drilling proponents. During the course of the cruise, actual site operations may indicate to the Co-Chief Scientists, the Expedition Project Manager/Staff Scientist, and the Operations Superintendent that it would be scientifically or operationally advantageous to amend the plan detailed in this prospectus. It should be understood that any substantial changes to the science deliverables outlined in the plan presented here are contingent upon the approval of the IODP JRSO Director and/or *JOIDES Resolution* Facility Board.

Disclaimer

Copyright

Citation

Planke, S., Berndt, C., and Alvarez Zarikian, C.A., 2021. *Expedition 396 Scientific Prospectus: Mid-Norwegian Continental Margin Magmatism*. International Ocean Discovery Program. https://doi.org/10.14379/iodp.sp.396.2021

ISSN

World Wide Web: 2332-1385

February 2021

Abstract

Volcanic passive margins are an end-member of continental rifted margins and are believed to originate from the breakup of a continent under the influence of a mantle plume. In spite of 40 y of research into this phenomenon, it is still unknown how excess magmatism is produced and what controls its surprisingly short duration. Expedition 396 will revisit the mid-Norwegian margin 36 y after Ocean Drilling Program Leg 104. It will provide the necessary observations to parameterize comprehensive 3-D numerical models. These will allow us to identify the relative importance of different tectonomagmatic processes. Furthermore, drilling will test the predictions of volcanic seismic facies models and elucidate the role of breakup volcanism in rapid global warming. Secondary objectives relate to the onset of the meridional overturning circulation in the North Atlantic Gateway and the potential to use the breakup basalt province to store carbon dioxide on industrial scales. To this end, Expedition 396 will attempt to drill nine boreholes on the Vøring and Møre margins. They will target the breakup volcanic successions as well as the overlying postrift sediments and the underlying synrift sediments. In conjunction with the wealth of reflection seismic data collected by the hydrocarbon industry during the past 40 y, the new borehole information will provide an unprecedented picture of the formation of a large igneous province during the opening of an ocean basin.

Schedule for Expedition 396

International Ocean Discovery Program (IODP) Expedition 396 is based on IODP drilling Proposal 944-Full2 and 944-Add2 (available at **http://iodp.tamu.edu/scienceops/expeditions/norwegian_continental_margin_magmatism.html**). Following evaluation by the IODP Scientific Advisory Structure, the expedition was scheduled for the research vessel (R/V) *JOIDES Resolution*, operating under contract with the *JOIDES Resolution* Science Operator (JRSO). At the time of publication of this *Scientific Prospectus*, the expedition is scheduled to start in Reykjavík, Iceland, on 6 August 2021 and to end in Kristiansand, Norway, on 6 October. A total of 61 days will be available for the transit, drilling, coring, and downhole measurements described in this report (for the current detailed schedule, see **http://iodp.tamu.edu/scienceops**). Further details about the facilities aboard *JOIDES Resolution* can be found at **http://iodp.tamu.edu/labs/index.html**.

Introduction

Continental extension, breakup, and the formation of new mid-oceanic spreading centers are fundamental parts of the plate tectonic cycle and have wide implications for the global environment (Berndt et al., 2019). Passive rifted margin studies have been at the core of the international ocean drilling program since the 1960s. Deep Sea Drilling Project (DSDP) and Ocean Drilling Program (ODP) drilling, along with extensive seismic surveying of the northeast Atlantic conjugate margins, demonstrated anomalously high volumes of volcanic activity during continental breakup, classifying these margins as “volcanic rifted margins” (Talwani and Eldholm, 1977; Eldholm et al., 1989a, 1989b; Saunders et al., 1998; Sengör and Burke, 1978; Ziegler and Cloetingh, 2004; Abdelmalak et al., 2016a, 2016b).

Expedition 396 builds on previous successful drilling campaigns in the northeast Atlantic—DSDP Leg 38 (1974) and ODP Legs 104 (1985), 152 (1993), and 163 (1995) (Figure **F1**)—that were instrumental in developing the concepts of volcanic rifted margins and large igneous provinces (LIPs) (see Mahoney and Coffin [1997] and Ernst [2014] for a summary). There are, however, many unresolved scientific questions related to formation and environmental implications of massive breakup volcanism that can be resolved by future scientific drilling. Meanwhile, comprehensive 3-D seismic data, new aeromagnetic data acquisition, seabed surveys, analysis of existing ODP data, and new scientific development during the past decade have led to a vastly improved proposal and drilling strategy. In particular, the paleoenvironmental objectives have been substantiated, and an independent application (Volcanic Forcing and Paleogene Climate Change; PVOLC) has been submitted to the International Continental Scientific Drilling Program (ICDP) for drilling Paleogene sediments in Denmark to resolve North Atlantic Igneous Province (NAIP) eruptions and environmental impact in a more distal setting.

Despite unsurpassed constraints on conjugate crustal structure between the northeast Atlantic Norwegian, Jan Mayen, and Greenland rifted margins, the mechanisms responsible for rift-related, anomalous excess magmatic productivity are still debated (Lundin and Doré, 2005; Brown and Lesher, 2014; Foulger et al., 2020). The controversy centers on three competing hypotheses:

1. Excess magmatism derived from elevated mantle potential temperatures resulting from mantle plume processes.
2. Small-scale convection at the base of the lithosphere enhanced the flux of material through the melt window during rifting and breakup.
3. Mantle source heterogeneity contributed to anomalously high melt production during continental breakup.

Although the mantle plume mechanism requires anomalous high temperatures resulting in high degrees of melting during asthenosphere upwelling, small-scale convection at the base of the lithosphere operates without elevated potential temperatures and is inherently connected to the rifting process (Boutilier and Keen, 1999).

Temporal correlations between mass extinctions, global warming, and formation of LIPs have long been recognized (Vogt, 1972; Wignall, 2001). However, the mechanisms for the rapid paleoenvironmental crises are highly debated in scientific literature (Bond and Wignall, 2014; Courtillot and Renne, 2003). For example, volcanic eruptions release large volumes of sulfur, halogens, and carbon to the atmosphere (Jones et al., 2016), which may cause environmental disturbances on a variety of timescales. An alternative, although not mutually exclusive mechanism, is that large volumes of greenhouse gases can be released from metamorphic aureoles around sill intrusions emplaced in sedimentary basins (Svensen et al., 2004). New information on eruption styles, volumes and rates, and sedimentological data in a proximal region to the eruptions is important to document and understand the environmental impact of LIP emplacement.

Background

Scientific drilling of northeast Atlantic continental margins since the 1970s has been essential for understanding the architecture and implications of igneous deposits associated with continental breakup. In particular, drilling of deep boreholes in the feather edge of the seaward-dipping reflectors (SDRs) offshore mid-Norway and southeast Greenland (Eldholm et al., 1989b; Larsen, Saunders, Clift, et al., 1994; Duncan, Larsen, Allan, et al., 1996; Saunders et al., 1998; Larsen et al., 1999) demonstrated that voluminous subaerial volcanic flows are common along rifted margins (Figure **F2**). The drilling results further suggested that continental breakup magmatism has had a major impact on the global environment and mass extinctions (Hinz, 1981; Eldholm and Thomas, 1993). Interpretation of industry seismic and borehole data from the Vøring Basin later led to the hypothesis that voluminous intrusion of magma in the organic-rich sedimentary basin may have triggered the Paleocene/Eocene Thermal Maximum (PETM) by release of aureole gases through hydrothermal vent complexes (Svensen et al., 2004). This hypothesis will be tested during Expedition 396.

Breakup volcanism along rifted passive margins is highly variable in both time and space. Mantle melting during the formation of mid-oceanic ridges is relatively well understood and mostly a function of spreading rate and mantle potential temperature with melting below the mid-oceanic ridge. It leads to accretion of 6–8 km of magmatic crust at standard mantle potential temperature and full spreading rates larger than 2 cm/y (Bown and White, 1994). On the other hand, factors controlling magmatic activity during continental rifting and breakup are not well known. The variation in the degree of magmatism at rifted margins can, to the first order, be characterized in three contrasting modes of behavior (Figure **F3**) (e.g., Huismans and Beaumont, 2011, 2014). Mode 1 margins are characterized by a sharp transition from the continent/ocean boundary (COB) to normal thickness (6–8 km) magmatic ocean crust. At Mode 2 margins, magmatic productivity exceeds that expected from decompression melting at normal mantle temperature. Mode 3 margins have little to no magmatism at the COB and a broad transition zone with a magmatic-exposed mantle at the seafloor preceding formation of mature oceanic crust.

A comprehensive understanding of what controls this range of behaviors and the volume, distribution, and timing of magmatism during continental rifting and breakup is, however, lacking. Excess magmatism at volcanic Mode 2 margins, such as in the northeast Atlantic, has been related to mantle plume and contrasting nonplume mechanisms (McKenzie and Bickle, 1988; Mutter et al., 1988; White and McKenzie, 1989).

Continental breakup may be associated with extensive volcanism over large distances along strike of the rifted margins as exemplified in the northeast Atlantic (Figure **F1**). The causes for the anomalous magmatic activity and the implications on the paleoenvironment are, however, still debated. Magmatic products emplaced along these volcanic rifted margins have four major characteristics:

- Wedges of SDRs and associated volcanic seismic facies units interpreted to be massive subaerial and submarine lava flows and volcaniclastic sediments are found on both sides of the COB.
- Extensive sill and hydrothermal vent complexes are emplaced in organic-rich sedimentary basins along the incipient breakup axis.
- Thick high-velocity bodies are found in the lower crust along the COB and commonly interpreted to be magmatic underplated material.
- The magmatic crust at these margins often exceeds 20 km, more than three times as thick as normal oceanic crust produced by passive upwelling of normal potential temperature mantle.

It appears that volcanic rifted margins require mantle that is either (1) anomalously hot, (2) actively upwelling at rates higher than the plate half-spreading rate, (3) anomalously fertile, or (4) some combination of these factors.

Geological setting

The northeast Atlantic rift system developed as a result of a series of rift episodes succeeding the Caledonian orogeny that ultimately led to continental breakup and passive margin formation in the Paleocene–Eocene (Talwani and Eldholm, 1977; White and McKenzie, 1989; Skogseid et al., 2000; Abdelmalak et al., 2016a; Zastrozhnov et al., 2020). The mid-Norwegian margin is well covered by 2-D and 3-D reflection and refraction seismic surveys, potential field and heat flow data, and borehole data that allow a refined structural and stratigraphic framework (Figure **F4**) (Brekke, 2000; Gernigon et al., 2003, 2020; Mjelde et al., 2005; Breivik et al., 2006; Theissen-Krah et al., 2017; Zastrozhnov et al., 2018, 2020; Polteau et al., 2020).

The mid-Norwegian margin is segmented by the northwest-trending Jan Mayen Fracture Zone, which separates the Møre and Vøring margins (Figures **F1**, **F4**). The margin segments are characterized by different tectonomagmatic style and sediment distribution (Berndt et al., 2001a; Gernigon et al., 2020). The largest magmatic accumulation is observed in the Vøring segment, and volumes decrease to the south and north. In the southern segment, passive margin formation and oceanic spreading was accommodated by the Aegir Ridge between the Møre and Jan Mayen (at the time connected to Greenland) conjugate margins in the Paleocene–Eocene.

Rifting and passive margin formation in the northeast Atlantic was accompanied by strong volcanic activity (White and McKenzie, 1989; Eldholm and Grue, 1994; Larsen and Saunders, 1998; Wright et al., 2012). Evidence for extensive magmatism is provided by SDRs, magmatic intrusions, and high-velocity bodies at the base of the continental crust underlying the COB, which in the distal margin are unequivocally interpreted to be magmatic underplate (Figures **F2**, **F5**) (Berndt et al., 2001a; Mjelde et al., 2005; Planke et al., 2005).

ODP drilling of the Vøring margin (Leg 104) and off southeast Greenland (Legs 152 and 163) recovered volcanic rock successions erupted during the initial stages of opening of the northeast Atlantic. Drilled rocks (Legs 152 and 163) range from prebreakup continental tholeiitic flood basalt to synbreakup picrites to oceanic-type basalts that form the main part of the SDRs (Fitton et al., 2000). Oceanic-type lavas show increasing degree of melting and contribution from asthenospheric mantle sources with time (Fram et al., 1998; Fitton et al., 1998). Thickness of igneous crust accreted at the southeast Greenland COB increases from about 18 km in the south to about 30 km near the Greenland-Iceland Rise (Holbrook et al., 2001). Similarly, geochemical enrichment of volcanics of the East Greenland margin (chondrite-normalized $[Ce/Y]_N$ and isotopes; Fitton et al., 1998; Tegner et al., 1998; Brown and Lesher, 2014) increases from south to north.

Correlation of crustal thickness and compositional enrichment suggests a combination of changes in source composition, source temperature, and/or melting dynamics. It is not known if a similar correlation of crustal thicknesses and magma compositions exists along the Norwegian margin. To establish the relationship between chemistry of the volcanics and crustal configuration is a milestone of the proposed investigations. Geochemical data show strong chemical and isotopic similarities between the "upper series" from the Vøring Plateau and southeast Greenland. In contrast, the "lower series" from both areas are fundamentally different from each other in many aspects, pointing to either substantial differences in prebreakup lithosphere composition at the two localities or different styles of mantle–crust interaction (Abdelmalak et al., 2016a).

Periods of elevated magmatism such as the emplacement of the NAIP often coincide with considerable environmental perturbations such as the PETM (56 Ma) and/or long-term climate warming such as the Early Eocene Climatic Optimum (EECO; ~50–53 Ma), suggesting a causal relationship (Figure **F6**) (Bond and Wignall, 2014; Eldholm and Thomas, 1993). The total volume of magma emplaced during the Paleogene is estimated to be 6 × 10^6 through 10 × 10^6 km^3 (Saunders et al., 2007; Horni et al., 2017), with the most voluminous activity roughly coinciding with the Paleocene/Eocene boundary (Storey et al., 2007a), although the full emplacement spans several million years (Wilkinson et al., 2017). Greenhouse gas emissions were likely generated by magmatic degassing (Storey et al., 2007b; Gutjahr et al., 2017) and by explosive discharge of thermogenic gases generated by contact metamorphism (Svensen et al., 2004; Frieling et al., 2016; Aarnes et al., 2010). Therefore, the emplacement of the NAIP is one of the primary contenders for instigating numerous hyperthermal events and long-term warming in the Paleogene, either as a direct forcing or as an instigator of positive climate feedbacks such as methane hydrate melting.

Seismic studies and site survey data

The supporting site survey data for Expedition 396 are archived at the IODP Site Survey Data Bank (**https://ssdb.iodp.org/SSDBquery/SSDBquery.php**; select 944 for proposal number) and shown in **Site summaries**.

The Norwegian continental shelf is covered by a high density of industry standard seismic and geophysical data in regions opened for petroleum exploration (Figure **F4**). The majority of the sites are located on industry-quality 3-D seismic data (Figure **F7**), including the sites on Kolga High and North Modgunn (AMN17 3-D cube) and Skoll High (CVX1101 3-D cube). The other sites are located on industry-quality 2-D data (Mimir High; MNR 2-D data) and outer Vøring margin (Outer High and Outer SDR; HV96 2-D data). See Table **T1** for a summary. For some of these sites, crossing lines are not always available exactly at the site.

High-resolution seismic P-Cable 3-D (two cubes of a total of 30 km^2) and 2-D (400 line km) data were acquired in August 2020 in the Kolga–Modgunn–Mimir region during the CAGE20-4-HH cruise. The cruise was a collaboration between the University of Oslo and the University of Tromsø and was supported by the Norwegian Petroleum Directorate. The data were collected near primary and alternate Expedition 396 sites. Other data collected during this cruise include multibeam echo sounder data, subbottom profiler data, gravity cores, and one conductivity-temperature-depth profiler data set. The data are currently being processed and will be available in early 2021.

Scientific objectives

The key objective of Expedition 396 is to understand the relationship between rifting, excess magmatism, and paleoclimate and to resolve the relative contribution from plume upwelling, small-scale convection, and mantle heterogeneity and their relation to the formation of volcanic rifted margins in the northeast Atlantic. This requires additional constraints on the following:

- Melting conditions (degree, pressure, and temperature of melting);
- Age distribution of volcanic products, which is essential to constrain magmatic productivity in time and space;
- Variation of pre-, syn-, and postbreakup magmatic activity across the margin;
- Variation of magmatic activity along strike across the major Møre and Vøring margin segments;
- Eruption rates, environment, and basalt morphologies; and
- The relationship between climate change, timing, volume, and style of magma emplacement.

The sedimentary proxy-based environmental reconstruction also provides a semiquantitative record of paleoelevations (water depth) and vertical motions as early rifting progresses to seafloor spreading, with the potential additional influence of dynamic support originating from the plume-pulsing hypothesis (e.g., Champion et al., 2008; Parnell-Turner et al., 2014).

The mid-Norwegian margin is among the best-studied volcanic rifted margins around the world. It has unsurpassed geophysical data coverage because of excellent collaboration between government, industry, and academia in Norway (Figure **F4**) and can be considered the type example of volcanic margins (Eldholm et al., 1995, 2002). However, key questions regarding the origin and implications of excess magmatism along with margin segmentation and rifting remain. Sampling of breakup volcanic successions and proximal sediment cores through IODP drilling, in conjunction with geochemical constraints on melt conditions and integrated quantitative models of melting and mantle convection, is crucial to advance our understanding of breakup processes and resolve competing hypotheses for excess magmatism and paleoenvironmental consequences.

The conjugate Norwegian–Jan Mayen–Greenland margin system is characterized by extensive breakup volcanism recorded as sill intrusions, flood basalt sequences, hyaloclastite buildups, and magmatic underplating (Figures **F1**, **F2**). Three main hypotheses for the formation of these massive magmatic constructions are related to a mantle plume, nonmantle plume active upwelling, or an enriched source scenario. A related hypothesis aims to constrain the influence of this extensive volcanic activity on Paleogene global climate. A combined interpretation of existing geophysical data, well data, and dredging samples cannot confidently distinguish between the proposed hypotheses. New core data will provide the required high-resolution insights into magmatic evolution in time.

The mid-Norwegian margin is a unique area in which well-characterized volcanic features, related to volcanic rifted margins worldwide, are readily drillable (Figures **F5**, **F7**). Here, igneous rocks and Paleogene sediments are locally buried by minor postbreakup sediments. Large regions along the outer margins have recently been covered by industry 3-D seismic surveys, and this unique database allows the identification of shallow (<200 meters below seafloor [mbsf]) volcanic and Paleogene sedimentary targets.

Although both volcanism and contact metamorphism degassing appear to coincide with the global warming events in the early Paleogene, considerable unknowns in terms of temporal volcanic development and potential gas fluxes from these sources remain. Moreover, with the presently available material it is difficult to separate the effects of volcanism and contact metamorphism and assess their relative forcing on the climate system. The acquisition of a core through continuous strata in close proximity to the NAIP would be an invaluable asset in deciphering the absolute and relative importance of these two processes (Figure **F6**). Although both volcanism and contact metamorphism release greenhouse gases (CO_2 and CH_4), the latter is likely to be rich in organic material and should therefore have a different stable carbon isotope signature ($\delta^{13}C$) to mantle-derived carbon. Differences in eruption style and location (e.g., subaerial vs. submarine) may impact the volume dispersal of metals used as volcanic proxies, such as mercury (Sanei et al., 2012). There may also be a systematic temporal evolution in the magmatic system, such as a shift from eruptive to intrusive activity (e.g., Burgess et al., 2017). Better age constraints on the eruptive stratigraphy and on subvolcanic rocks in proximity to hydrothermal vent complexes may resolve potential diachroneities and shed light on degassing mechanisms responsible for climatic perturbations.

The following are the main scientific objectives for Expedition 396:

1. Determine the role of the Iceland plume in producing excess magma along the mid-Norwegian segment of the northeast Atlantic volcanic rifted margin during the Paleogene by constraining the conditions of melting (temperature, pressure, mantle sources, and total degree of melting).
2. Determine the cause for along-axis variation in melt production. In the case of the northeast Atlantic volcanic margins, magmatic productivity changes from the Møre margin (~12–15 km thick magmatic crust) in the south toward the Vøring margin (>20 km thick magmatic crust) and the Lofoten margin (~8 km regular thickness magmatic crust). This pattern suggests a local, structural control because plume models would suggest largest excess magmatic activity in the southernmost conjugate sections (e.g., Møre–Jan Mayen) closest to the Iceland thermal anomaly.
3. Determine the depositional environment (subaerial vs. submarine) of inner and outer lava flows (e.g., SDRs) and implications for vertical motions during late synrift, breakup, and early postrift oceanic spreading. Some of the lava flows may not have extruded subaerially (e.g., Planke et al., 2000, 2017). This has important implications for the distribution of buoyancy forces and isostasy during breakup where sections without continental crust would under normal conditions be expected at water depths >2 km (e.g., Kusznir et al., 2004).
4. Determine the timing of magmatic activity and document the occurrence and temporal evolution of paleoclimate and volcanic proxies in sedimentary sequences proximal to the NAIP.
5. Use the integrated paleoclimate and paleoenvironment proxies and geochronological data to assess the relative importance of volcanism and thermogenic release from hydrothermal vent complexes as potential drivers of climate change events.

Furthermore, there are two secondary scientific objectives:

1. Early Eocene hothouse and freshwater incursions into the North Atlantic. The early Paleogene (~66–45 Ma) was characterized by warm global greenhouse conditions culminating in the EECO (~53–50 Ma), the warmest sustained climates of the last 65 My (Bijl et al., 2009; Anagnostou et al., 2016; Cramwinckel et al., 2018), inducing an intensified hydrological cycle with strongly increased precipitation at high latitudes (e.g., Pagani et al., 2006; Suan et al., 2017). Paleogene sediments obtained during Integrated Ocean Drilling Program Expedition 302 (Arctic Coring Expedition) show large quantities of free-floating freshwater Azolla, which grew and reproduced in the Arctic Ocean by the onset of the middle Eocene (~48 Ma) (Brinkhuis et al., 2006). The proposed sites penetrate the Eocene sediments and allow testing of the extent of freshwater incursions, constraining paleoceanographic boundary conditions for the excursions, including the evolution of oceanic gateways and their influence on global ocean circulation. The early Eocene sediments also provide a unique opportunity to reconstruct mid–high northern latitude climate, allowing a detailed comparison to Southern Ocean records (e.g., Bijl et al., 2009, 2013; Hollis et al., 2012).
2. Carbon capture and storage in basalt provinces. Observations of meteoric water and high dissolved calcium concentration from the bottom of ODP Sites 642 and 643 show that the Vøring Plateau is ideal for studying circulation of freshwater within such large basaltic formations and assessing its potential for CO_2 sequestration. Previous ODP holes did not address the origin of meteoric water and trigger(s) for such large-scale circulation. Dating of borehole water samples with ^{14}C, ^{36}Cl, and $^{234}U/^{238}U$ tracers and systematic analyses of fluid geochemistry (Inagaki et al., 2015) will allow the determination of the source of meteoric waters and provide constraints on their circulation systems, which are crucial for assessing the CO_2 storage potential of breakup basalts. Pore fluids will be sampled along the complete proposed drilling transect to investigate the potential extent of meteoric water flow. We hypothesize that meteoric water will be detected at the sites reaching the basaltic basement (e.g., Proposed Sites VMVM-20A, VMVM-23A, VMVM-61A, and VMVM-07A) but will be absent from the sites that do not reach basement (e.g., Proposed Sites VMVM-31A, VMVM-40A, and VMVM-55B). The outcome of fluid geochemical analyses will be quantitatively interpreted with hydrological modeling using software such as MODFLOW to investigate the flow path of meteoric water. The sampling for water geochemistry will follow the standard IODP protocol for pore fluid analyses.

Operations plan and coring strategy

The mid-Norwegian margin is the type locality for volcanic rifted margins and is probably the best-studied volcanic margin worldwide. The detailed geometry and amount of volcanic products in the form of underplated bodies and intrusive and extrusive volcanic rocks are currently extremely well constrained through geophysical imaging (e.g., Mjelde et al., 2005; Berndt et al., 2001b; Planke et al., 2017; Abdelmalak et al., 2016a, 2016b, 2017). However, new information on the age, nature, and depositional environment of the volcanic rocks is required to constrain melt production rates and vertical motions. Furthermore, causes for excess magmatic productivity are not well understood and highly debated.

Answering the fundamental questions outlined in the scientific objectives requires extensive sampling of both late synrift/early postrift sediments and magmatic products from the continental into the oceanic domain (Figure **F7**). Collection of sedimentary records proximal to the volcanic and magmatic activity allows for use of numerous proxies to distinguish between volcanic and hydrothermal vent complex sources.

Geochemical, geochronological, and petrological analyses of drilled volcanic rocks and sediments will provide constraints on the timing of magmatism relative to rifting and breakup, the conditions of melting (pressure, temperature, composition of the source, and degree of melting), the volcanic emplacement environment (subaerial vs. subaqueous), and paleoenvironmental changes. Ocean drilling provides the only means of obtaining these samples and is therefore essential for meeting these objectives.

Access to modern industry standard 2-D and 3-D seismic data has been particularly important for optimizing the drill site locations (Figure **F5**). Nine primary sites were selected for the initial proposal, but some sites were later slightly shifted to address the IODP Science Evaluation Panel and Environmental Protection and

Safety Panel (EPSP) review comments. A number of alternative sites were also identified, normally in close vicinity to the primary sites.

In total, 26 sites are proposed (see **Site summaries**). Because of government safety regulations, most sites are approved to less than 200 m deep. This is a limit normally applied for geotechnical and stratigraphic drilling in sedimentary basin environments in Norway. Some proposed sites in the oceanic domain or near the COB have deeper penetration, notably Sites VMVM-55B (800 m), VMVM-09A (550 m), and VMVM-10B (750 m). Deeper scientific holes were drilled previously in the same region (e.g., Hole 642E [1229 mbsf], Site 643 [565 mbsf], and DSDP Site 341 [456 mbsf]).

Proposed drill sites

The drilling strategy for the proposed boreholes is summarized in Figure **F7** and Table **T2**. The coring and logging tools available on *JOIDES Resolution* are described at **http://iodp.tamu.edu/tools** and **http://iodp.tamu.edu/tools/logging**. The drilling plan will provide one along-strike and one cross-strike margin transect and two high-resolution Paleogene sedimentary sites.

1. The subbasalt and initial volcanic flows are the targets of Proposed Sites VMVM-20A and VMVM-23A. If successful, these will be the first boreholes to sample prebreakup volcanics and the onset basalt flows on the mid-Norwegian margin.
2. Paleogene sediments in hydrothermal vent complexes and sedimentary reference holes across the Paleocene/Eocene boundary are the targets of Proposed Sites VMVM-31A, VMVM-40B, and VMVM-55B. These sites will, for the first time, document the nature of hydrothermal vent complexes in the outer Vøring Basin and provide geochemical proxy data and age constraints for the Paleogene succession. We propose dual coring of key stratigraphic intervals. For Proposed Site VMVM-55B, one deep hole (800 m) is proposed, whereas four offset holes of 200 m each along a ribbon with outgoing strata is an alternative drilling strategy (Proposed Site VMVM-56A ribbon) (Figure **F7**).
3. Sampling of volcanic seismic facies units across the central Vøring margin to assess the spatial and temporal development of the breakup volcanic complex is planned for Proposed Sites VMVM-61A, VMVM-07A, VMVM-80A, and VMVM-09A. These sites will be integrated with results from existing scientific boreholes, such as Hole 642E. The focus is on understanding the emplacement environment, characterizing sequence boundaries, and sampling of basalt for geochemical and geochronological studies.
4. In addition, Site 642 may be revisited to measure borehole temperature and acquire complementary wireline data.

Standard *JOIDES Resolution* drilling and logging procedures will be followed. For the six sites with a volcanic basement target, one rotary core barrel (RCB) hole will be drilled to bit destruction or total depth. We plan to get at least 50 m of basement penetration for all these sites, with a recovery of about 50%. Advanced piston corer (APC)/extended core barrel (XCB) drilling may be attempted for thick Quaternary–Neogene sediments at Proposed Sites VMVM-07A and VMVM-09A.

APC/XCB drilling also will be attempted to get higher recovery of Paleogene sediments at Proposed Sites VMVM-31A through VMVM-55B, particularly because high recovery from Proposed Sites VMVM-40B and VMVM-55B is important. However, RCB drilling will replace APC/XCB drilling if penetration of Paleogene sediments is difficult. Duplicate holes at the two key Paleogene sites (VMVM-40B and VMVM-55B) will be drilled across the Paleocene/Eocene boundary, if present.

Wireline logging and downhole measurements strategy

A comprehensive wireline logging program is planned for all sites. Two standard log runs are planned for all holes. Good borehole imaging logs (Formation MicroScanner [FMS] and Ultrasonic Borehole Imager [UBI]) are particularly important to characterize the basement sites where recovery of fractured and altered intervals is expected to be relatively low. The wireline logs are also very useful for core-log integration and the establishment of a high-resolution stratigraphy in both volcanic and sedimentary sequences (e.g., Planke, 1994; Jerram et al., 2019). Vertical seismic experiments (or check shot surveys) are planned for deep holes and some basement holes where core-log-seismic integration is important.

The drilling plan is to start with the Kolga High sites and then continue northwest across the Vøring Plateau sites and finally to the Lofoten Basin sites. As such, the sites are numbered in prioritized order. We do expect some downtime due to weather (particularly in September), and technical problems may cause us to skip some of the sites or reduce the logging program. In any circumstance, there should be a balance in time spent on basement- and stratigraphy-related sites.

Risks and contingency

The proposed sites are located in a region that has been studied extensively for commercial and scientific purposes; comprehensive seismic survey data are available; and a number of scientific, stratigraphic, and industry boreholes exist nearby. All site locations have been reviewed and approved by the EPSP. However, a number of key factors pose risks or potential hazards for this expedition, including the possible presence of hydrocarbons and gas hydrates, fluid overpressure, hard sedimentary layers (overburden), hard–soft basalt drilling, and weather. A detailed safety report was prepared for the EPSP and is available from JRSO.

This expedition will sail in the later part of the northern hemisphere summer, and sea-surface conditions can be rough in the North Atlantic. Therefore, adverse weather conditions, sea state, and the resulting heave can have adverse effects on drilling operations and can significantly affect core quality and recovery. It may also cause a significant loss of time.

Three different coring systems (APC, XCB, and RCB) will be used to ensure we meet the scientific objectives. At most sites, one RCB hole will be drilled to 200 mbsf, with the goal of sampling over 50 m of basement below. Duplicate holes are planned at two sites with Paleocene–Eocene stratigraphic targets (Proposed Sites VMVM-40B and VMVM-55B). These sites will be drilled/cored using the piston coring (APC/half-length APC [HLAPC]) and XCB systems to attempt to recover high-quality sequences suitable for high-resolution Paleocene paleoceanographic studies. The RCB system will be used in the second hole at Proposed Site VMVM-55B to achieve the deep penetration target depth of 800 mbsf.

It should be noted that open holes on the Norwegian continental margin normally may not be deeper than 200 m because of government safety regulations. However, there is precedent of scientific drilling of deep holes in the margin, and we believe that the Norwegian authorities will allow deeper drilling in this case. To address the potential limitations associated with reaching the 800 m deep target at Proposed Site VMVM-55B, we have envisioned a combination of a sequence of ribbon sites where key targets of Paleocene/post-Paleocene overburden sediments can be reached with shallow boreholes.

Other risks to the successful completion of the program include operational problems caused by lower than predicted penetration rates or unstable borehole conditions. Hole stability is always a risk during coring operations, and the risk is higher when there are longer sections of open (not cased) hole. Unconsolidated sediments may create unstable borehole conditions, in particular for reaching deep targets. Poor hole conditions, such as loose unconsolidated material or collapsing holes, can prevent our ability to penetrate deeply or successfully conduct logging. They can also lead to a stuck drill pipe. A stuck drill string is always a risk during coring operations and expedition time can be consumed while attempting to free the stuck drill string or, in the worst case, severing the stuck drill string. This can result in the complete loss of the hole and loss of equipment. *JOIDES Resolution* carries sufficient spare drilling equipment to enable the continuation of coring, but the time lost to the expedition can be significant. Hiatuses in the recovered sediments or incomplete sections may prevent the recovery of key sedimentary sections (e.g., the PETM) and result in not achieving all the scientific objectives.

Sampling and data sharing strategy

Shipboard and shore-based researchers should refer to the IODP Sample, Data, and Obligations Policy and Implementation Guidelines posted on the Web at **http://www.iodp.org/top-resources/program-documents/policies-and-guidelines**. This document outlines the policy for distributing IODP samples and data to research scientists, curators, and educators. The document also defines the obligations that sample and data recipients incur. The Sample Allocation Committee (SAC), composed of the Co-Chief Scientists, Staff Scientist, and IODP Curator on shore and curatorial representative on board the ship, will work with the entire scientific party to formulate a formal expedition-specific sampling plan for shipboard and postcruise sampling.

Shipboard scientists are expected to submit sample requests (at **http://iodp.tamu.edu/curation/samples.html**) ~6 months before the beginning of the expedition. Based on sample requests (shipboard and shore based) submitted by this deadline, the SAC will prepare a tentative sampling plan, which will be revised on the ship as dictated by core recovery and expedition objectives. The sampling plan will be subject to modification depending upon the actual material recovered and collaborations that may evolve between scientists during the expedition. Modifications of the sampling strategy during the expedition must be approved by the Co-Chief Scientists, Staff Scientist, and curatorial representative on board the ship.

The majority of the sampling for postcruise research will be postponed until a shore-based sampling party that will be implemented approximately 4–6 months after the end of the expedition at the Bremen Core Repository (BCR) in Bremen, Germany. All shipboard and approved shore-based scientists, students, and collaborators will be invited to help collect the thousands of anticipated samples. Sampling on the ship will consist of samples for shipboard measurements as well as personal research samples for ephemeral properties and hard rock. Although we will endeavor to collect as many of the hard rock samples on the ship as possible, some of the sampling may take place postcruise during the sampling party.

The minimum permanent archive will be the standard archive half of each core and will not be sampled. Following the expedition, the IODP Curator will finalize the selection of archive halves designated as permanent over any intervals recovered from multiple holes at a site. All sample frequencies and sample sizes/volumes must be justified on a scientific basis and will depend on core recovery, the full spectrum of other requests, and the expedition objectives. Some redundancy of measurement is unavoidable, but minimizing the duplication of measurements among the shipboard party and identified shore-based collaborators will be a factor in evaluating sample requests. Success will require collaboration, integration of complementary data sets, and consistent methods of analysis. Substantial collaboration and cooperation are highly encouraged.

There may be considerable demand for samples from a limited amount of cored material for some critical intervals. Critical intervals may require special handling, a higher sampling density, reduced sample size, or continuous core sampling for a set of particularly high-priority research objectives. The SAC may require an additional formal sampling plan before critical intervals are sampled, and a special sampling plan will be developed to maximize scientific return and scientific participation and to preserve some material for future studies. The SAC can decide at any stage during the expedition or during the 1 y moratorium period which recovered intervals should be considered critical.

Following Expedition 396, cores will be delivered to the BCR. However, the archive halves may be shipped to the IODP Gulf Coast Repository in College Station, Texas (United States), for postcruise programmatic X-ray fluorescence core scanning. Upon completion of these measurements, cores will be sent to the BCR for permanent storage.

All collected data and samples will be protected by a 1 y moratorium period following the completion of the postexpedition sampling party. During this time, data and samples will be available only to the Expedition 396 shipboard scientists and approved shore-based participants.

Expedition scientists and scientific participants

The current list of participants for Expedition 396 can be found at **http://iodp.tamu.edu/scienceops/expeditions/norwegian_continental_margin_magmatism.html**.

References

Aarnes, I., Svensen, H., Connolly, J.A.D., and Podladchikov, Y.Y., 2010. How contact metamorphism can trigger global climate changes: modeling gas generation around igneous sills in sedimentary basins. *Geochimica et Cosmochimica Acta*, 74(24):7179–7195. **https://doi.org/10.1016/j.gca.2010.09.011**

Abdelmalak, M.M., Faleide, J.I., Planke, S., Gernigon, L., Zastrozhnov, D., Shephard, G.E., and Myklebust, R., 2017. The T-reflection and the deep crustal structure of the Vøring margin, offshore mid-Norway. *Tectonics*, 36(11):2497–2523. **https://doi.org/10.1002/2017TC004617**

Abdelmalak, M.M., Meyer, R., Planke, S., Faleide, J.I., Gernigon, L., Frieling, J., Sluijs, A., Reichart, G.J., Zastrozhnov, D., Theissen-Krah, S., Said, A., and Myklebust, R., 2016a. Pre-breakup magmatism on the Vøring margin; insight from new sub-basalt imaging and results from Ocean Drilling Program Hole 642E. *Tectonophysics*, 675:258–274. **https://doi.org/10.1016/j.tecto.2016.02.037**

Abdelmalak, M.M., Planke, S., Faleide, J.I., Jerram, D.A., Zastrozhnov, D., Eide, S., and Myklebust, R., 2016b. The development of volcanic sequences at rifted margins: new insights from the structure and morphology of the Vøring escarpment, mid-Norwegian margin. *Journal of Geophysical Research: Solid Earth*, 121(7):5212–5236. **https://doi.org/10.1002/2015JB012788**

Abdelmalak, M.M., Planke, S., Polteau, S., Hartz, E.H., Faleide, J.I., Tegner, C., Jerram, D.A., Millett, J.M., and Myklebust, R., 2019. Breakup volcanism and plate tectonics in the NW Atlantic. *Tectonophysics*, 760:267–296. **https://doi.org/10.1016/j.tecto.2018.08.002**

Anagnostou, E., John, E.H., Edgar, K.M., Foster, G.L., Ridgwell, A., Inglis, G.N., Pancost, R.D., Lunt, D.J., and Pearson, P.N., 2016. Changing atmospheric CO_2 concentration was the primary driver of early Cenozoic climate. *Nature*, 533(7603):380–384. **https://doi.org/10.1038/nature17423**

Berndt, C., Mjelde, R., Planke, S., Shimamura, H., and Faleide, J.I., 2001a. Controls on the tectono-magmatic evolution of a volcanic transform margin: the Vøring transform margin, NE Atlantic. *Marine Geophysical Research*, 22:133–152. **https://doi.org/10.1023/A:1012089532282**

Berndt, C., Planke, S., Alvestad, E., Tsikalas, F., and Rasmussen, T., 2001b. Seismic volcanostratigraphy of the Norwegian margin: constraints on tectonomagmatic break-up processes. *Journal of the Geological Society (London, United Kingdom)*, 158(3):413–426. **https://doi.org/10.1144/jgs.158.3.413**

Berndt, C., Planke, S., Teagle, D., Huismans, R., Torsvik, T., Frieling, J., Jones, M.T., Jerram, D.A., Tegner, C., Faleide, J.I., Coxall, H., and Hong, W.-L., 2019. Northeast Atlantic breakup volcanism and consequences for Paleogene climate change – MagellanPlus Workshop report. *Scientific Drilling*, 26:69–85. **https://doi.org/10.5194/sd-26-69-2019**

Bijl, P.K., Bendle, J.A.P., Bohaty, S.M., Pross, J., Schouten, S., Tauxe, L., Stickley, C.E., McKay, R.M., Röhl, U., Olney, M., Sluijs, A., Escutia, C., and Brinkhuis, H., 2013. Eocene cooling linked to early flow across the Tasmanian Gateway. *Proceedings of the National Academy of Sciences of the United States of America*, 110(24):9645–9650. **https://doi.org/10.1073/pnas.1220872110**

Bijl, P.K., Schouten, S., Sluijs, A., Reichart, G.-J., Zachos, J.C., and Brinkhuis, H., 2009. Early Palaeogene temperature evolution of the southwest Pacific Ocean. *Nature (London)*, 461(7265):776–779. **https://doi.org/10.1038/nature08399**

Boldreel, L.O., and Andersen, M.S., 1994. Tertiary development of the Faroe-Rockall Plateau based on reflection seismic data. *Bulletin of the Geological Society of Denmark*, 41:162–180.

Bond, D.P.G., and Wignall, P.B., A.C., 2014. Large igneous provinces and mass extinctions: an update. *In* Keller, G. and Kerr, A.C. (Eds.), *Volcanism, Impacts, and Mass Extinctions: Causes and Effects.* Special Paper – Geological Society of America. **https://doi.org/10.1130/2014.2505(02)**

Boutilier, R.R., and Keen, C.E., 1999. Small-scale convection and divergent plate boundaries. *Journal of Geophysical Research: Solid Earth*, 104(B4):7389–7403. **https://doi.org/10.1029/1998JB900076**

Bown, J.W., and White, R.S., 1994. Variation with spreading rate of oceanic crustal thickness and geochemistry. *Earth and Planetary Science Letters*, 121(3):435–449. **https://doi.org/10.1016/0012-821X(94)90082-5**

Breivik, A.J., Mjelde, R., Faleide, J.I., and Murai, Y., 2006. Rates of continental breakup magmatism and seafloor spreading in the Norway Basin–Iceland plume interaction. *Journal of Geophysical Research: Solid Earth*, 111(B7):B07102. **https://doi.org/10.1029/2005JB004004**

Brekke, H., 2000. The tectonic evolution of the Norwegian Sea Continental Margin with emphasis on the Vøring and Møre Basins. *Geological Society Special Publication*, 167(1):327–378. **https://doi.org/10.1144/gsl.Sp.2000.167.01.13**

Brinkhuis, H., Schouten, S., Collinson, M.E., Sluijs, A., Damsté, J.S.S., Dickens, G.R., Huber, M., Cronin, T.M., Onodera, J., Takahashi, K., Bujak, J.P., Stein, R., van der Burgh, J., Eldrett, J.S., Harding, I.C., Lotter, A.F., Sangiorgi, F., Cittert, H.v.K.-v., de Leeuw, J.W., Matthiessen, J., Backman, J., Moran, K., and the Expedition Scientists, 2006. Episodic fresh surface waters in the Eocene Arctic Ocean. *Nature*, 441(7093):606–609. **https://doi.org/10.1038/nature04692**

Brown, E.L., and Lesher, C.E., 2014. North Atlantic magmatism controlled by temperature, mantle composition and buoyancy. *Nature Geoscience*, 7(11):820–824. **https://doi.org/10.1038/ngeo2264**

Burgess, S.D., Muirhead, J.D., and Bowring, S.A., 2017. Initial pulse of Siberian Traps sills as the trigger of the end-Permian mass extinction. *Nature Communications*, 8(1):164. **https://doi.org/10.1038/s41467-017-00083-9**

Chambers, L.M., Pringle, M.S., and Parrish, R.R., 2005. Rapid formation of the Small Isles Tertiary centre constrained by precise $^{40}Ar/^{39}Ar$ and U–Pb ages. *Lithos*, 79(3):367–384. **https://doi.org/10.1016/j.lithos.2004.09.008**

Champion, M.E.S., White, N.J., Jones, S.M., and Lovell, J.P.B., 2008. Quantifying transient mantle convective uplift: an example from the Faroe-Shetland Basin. *Tectonics*, 27(1):1–18. **https://doi.org/10.1029/2007TC002106**

Courtillot, V.E., and Renne, P.R., 2003. On the ages of flood basalt events. *Comptes Rendus Geoscience*, 335(1):113–140. **https://doi.org/10.1016/S1631-0713(03)00006-3**

Cramer, B.S., Toggweiler, J.R., Wright, J.D., Katz, M.E., and Miller, K.G., 2009. Ocean overturning since the Late Cretaceous; inferences from a new benthic foraminiferal isotope compilation. *Paleoceanography*, 24(4):PA4216. **https://doi.org/10.1029/2008PA001683**

Cramwinckel, M.J., Huber, M., Kocken, I.J., Agnini, C., Bijl, P.K., Bohaty, S.M., Frieling, J., Goldner, A., Hilgen, F.J., Kip, E.L., Peterse, F., van der Ploeg, R., Röhl, U., Schouten, S., and Sluijs, A., 2018. Synchronous tropical and polar temperature evolution in the Eocene. *Nature*, 559(7714):382–386. **https://doi.org/10.1038/s41586-018-0272-2**

Davison, I., Stasiuk, S., Nuttall, P., and Keane, P., 2010. Sub-basalt hydrocarbon prospectivity in the Rockall, Faroe–Shetland and Møre Basins, NE Atlantic. *Geological Society of London, Petroleum Geology Conference Series*, 7(1):1025–1032. **https://doi.org/10.1144/0071025**

Duncan, R.A., Larsen, H.C., Allan, J.F., et al., 1996. *Proceedings of the Ocean Drilling Program, Initial Reports,* 163: College Station, TX (Ocean Drilling Program). **https://doi.org/10.2973/odp.proc.ir.163.1996**

Eldholm, O., and Grue, K., 1994. North Atlantic volcanic margins: dimensions and production rates. *Journal of Geophysical Research: Solid Earth*, 99(B2):2955–2968. **https://doi.org/10.1029/93JB02879**

Eldholm, O., Skogseid, J., Planke, S., and Gladczenko, T.P., 1995. Volcanic margin concepts. *NATO ASI Series, Series C: Mathematical and Physical Sciences*, 463:1–16. **https://doi.org/10.1007/978-94-011-0043-4_1**

Eldholm, O., Thiede, J., and Taylor, E., 1989a. Evolution of the Norwegian continental margin; background and objectives. *In* Duncan, R.A., Larsen, H.C., Allan, J.F., et al., *Proceedings of the Ocean Drilling Program, Scientific Results*, 104: College Station, TX (Ocean Drilling Program), 5–26. **https://doi.org/10.2973/odp.proc.sr.104.191.1989**

Eldholm, O., Thiede, J., and Taylor, E., 1989b. The Norwegian continental margin: tectonic, volcanic, and paleoenvironmental framework. *In* Eldholm, O., Thiede, J., and Taylor, E., et al., *Proceedings of the Ocean Drilling Program, Scientific Results*, 104: College Station, TX (Ocean Drilling Program), 5–26. **https://doi.org/10.2973/odp.proc.sr.104.110.1989**

Eldholm, O., and Thomas, E., 1993. Environmental impact of volcanic margin formation. *Earth and Planetary Science Letters*, 117(3–4):319–329. **https://doi.org/10.1016/0012-821X(93)90087-P**

Eldholm, O., Tsikalas, F., and Faleide, J.I., 2002. Continental margin off Norway 62–75°N: Palaeogene tectono-magmatic segmentation and sedimentation. *Geological Society Special Publications*, 197(1):39–68. **https://doi.org/10.1144/GSL.SP.2002.197.01.03**

Elliott, G.M., and Parson, L.M., 2008. Influence of margin segmentation upon the break-up of the Hatton Bank rifted margin, NE Atlantic. *Tectonophysics*, 457(3):161–176. **https://doi.org/10.1016/j.tecto.2008.06.008**

Ernst, R.E., 2014. *Large Igneous Provinces:* Cambridge, UK (Cambridge University Press). **https://doi.org/10.1017/CBO9781139025300**

Fitton, J.G., Larsen, L.M., Saunders, A.D., Hardarson, B.S., and Kempton, P.D., 2000. Palaeogene continental to oceanic magmatism on the SE Greenland continental margin at 63°N; a review of the results of Ocean Drilling Program Legs 152 and 163. *Journal of Petrology*, 41(7):951–966. **https://doi.org/10.1093/petrology/41.7.951**

Fitton, J.G., Saunders, A.D., Larsen, L.M., Hardarson, B.S., and Norry, M.J., 1998. Volcanic rocks from the Southeast Greenland margin at 63°N; composition, petrogenesis, and mantle sources. *In* Saunders, A.D., Larsen, H.C., and Wise, S.W., Jr. (Eds.), *Proceedings of the Ocean Drilling Program, Scientific Results*, 152: College Station, TX (Ocean Drilling Program), 331–350. **https://doi.org/10.2973/odp.proc.sr.152.233.1998**

Foulger, G.R., Doré, T., Emeleus, C.H., Franke, D., Geoffroy, L., Gernigon, L., Hey, R., Holdsworth, R.E., Hole, M., Höskuldsson, Á., Julian, B., Kusznir, N., Martinez, F., McCaffrey, K.J.W., Natland, J.H., Peace, A.L., Petersen, K., Schiffer, C., Stephenson, R., and Stoker, M., 2020. The Iceland microcontinent and a continental Greenland-Iceland-Faroe Ridge. *Earth-Science Reviews*, 206:102926. **https://doi.org/10.1016/j.earscirev.2019.102926**

Fram, M.S., Lesher, C.E., and Volpe, A.M., 1998. Mantle melting systematics; transition from continental to oceanic volcanism on the southeast Greenland margin. *In* Saunders, A.D., Larsen, H.C. and Wise, S.W., Jr. (Eds.), *Proceedings of the Ocean Drilling Program, Scientific Results*, 152: College Station, TX (Ocean Drilling Program), 373–386. **https://doi.org/10.2973/odp.proc.sr.152.236.1998**

Frieling, J., Svensen, H.H., Planke, S., Cramwinckel, M.J., Selnes, H., and Sluijs, A., 2016. Thermogenic methane release as a cause for the long duration of the PETM. *Proceedings of the National Academy of Sciences of the United States of America*, 113(43):12059–12064. **https://doi.org/10.1073/pnas.1603348113**

Ganerød, M., Chew, D.M., Smethurst, M.A., Troll, V.R., Corfu, F., Meade, F., and Prestvik, T., 2011. Geochronology of the Tardree Rhyolite Complex, Northern Ireland: implications for zircon fission track studies, the North Atlantic Igneous Province and the age of the Fish Canyon sanidine standard. *Chemical Geology*, 286(3):222–228. **https://doi.org/10.1016/j.chemgeo.2011.05.007**

Ganerød, M., Smethurst, M.A., Torsvik, T.H., Prestvik, T., Rousse, S., McKenna, C., Van Hinsbergen, D.J.J., and Hendriks, B.W.H., 2010. The North Atlantic Igneous Province reconstructed and its relation to the Plume Generation Zone: the Antrim Lava Group revisited. *Geophysical Journal International*, 182(1):183–202. **https://doi.org/10.1111/j.1365-246X.2010.04620.x**

Geissler, W.H., Gaina, C., Hopper, J.R., Funck, T., Blischke, A., Arting, U., Horni, J.A., Péron-Pinvidic, G., and Abdelmalak, M.M., 2016. Seismic volcanostratigraphy of the NE Greenland continental margin. *Geological Society Special Publication*, 447(1):149–170. **https://doi.org/10.6084/m9.figshare.c.3593780**

Gernigon, L., Franke, D., Geoffroy, L., Schiffer, C., Foulger, G.R., and Stoker, M., 2020. Crustal fragmentation, magmatism, and the diachronous opening of the Norwegian-Greenland Sea. *Earth-Science Reviews*, 206:102839. **https://doi.org/10.1016/j.earscirev.2019.04.011**

Gernigon, L., Ringenbach, J.C., Planke, S., Gall, B.L., and Jonquet-Kolstø, H., 2003. Extension, crustal structure and magmatism at the outer Vøring Basin, Norwegian margin. *Journal of the Geological Society*, 160(2):197–208. **https://doi.org/10.1144/0016-764902-055**

Gutjahr, M., Ridgwell, A., Sexton, P.F., Anagnostou, E., Pearson, P.N., Palike, H., Norris, R.D., Thomas, E., and Foster, G.L., 2017. Very large release of mostly volcanic carbon during the Palaeocene-Eocene Thermal Maximum. *Nature (London)*, 548(7669):573–577. **https://doi.org/10.1038/nature23646**

Hamilton, M.A., Pearson, D.G., Thompson, R.N., Kelley, S.P., and Emeleus, C.H., 1998. Rapid eruption of Skye lavas inferred from precise U–Pb and Ar–Ar dating of the Rum and Cuillin plutonic complexes. *Nature*, 394(6690):260–263. **https://doi.org/10.1038/28361**

Hinz, K., 1981. A hypothesis on terrestrial catastrophes wedges of very thick oceanward dipping layers beneath passive continental margins; their origin and paleoenvironmental significance. *Geologisches Jahrbuch, Reihe E: Geophysik*, 22:3–28.

Holbrook, W.S., Larsen, H.C., Korenaga, J., Dahl-Jensen, T., Reid, I.D., Kelemen, P.B., Hopper, J.R., Kent, G.M., Lizarralde, D., Bernstein, S., and Detrick, R.S., 2001. Mantle thermal structure and active upwelling during continental breakup in the North Atlantic. *Earth and Planetary Science Letters*, 190(3):251–266. **https://doi.org/10.1016/S0012-821X(01)00392-2**

Hollis, C.J., Taylor, K.W.R., Handley, L., Pancost, R.D., Huber, M., Creech, J.B., Hines, B.R., Crouch, E.M., Morgans, H.E.G., Crampton, J.S., Gibbs, S., Pearson, P.N., and Zachos, J.C., 2012. Early Paleogene temperature history of the southwest Pacific Ocean; reconciling proxies and models. *Earth and Planetary Science Letters*, 349–350:53–66. **https://doi.org/10.1016/j.epsl.2012.06.024**

Horni, J.Á., Hopper, J.R., Blischke, A., Geisler, W.H., Stewart, M., McDermott, K., Judge, M., Erlendsson, Ö., and Árting, U., 2017. Regional distribution of volcanism within the North Atlantic Igneous Province. *Geological Society Special Publications*, 447(1):105–125. **https://doi.org/10.1144/SP447.18**

Huismans, R., and Beaumont, C., 2011. Depth-dependent extension, two-stage breakup and cratonic underplating at rifted margins. *Nature*, 473(7345):74–78. **https://doi.org/10.1038/nature09988**

Huismans, R.S., and Beaumont, C., 2014. Rifted continental margins: The case for depth-dependent extension. *Earth and Planetary Science Letters*, 407:148–162. **https://doi.org/10.1016/j.epsl.2014.09.032**

Inagaki, F., Hinrichs, K.U., Kubo, Y., Bowles, M.W., Heuer, V.B., Hong, W.L., Hoshino, T., Ijiri, A., Imachi, H., Ito, M., Kaneko, M., Lever, M.A., Lin, Y.S., Methé, B.A., Morita, S., Morono, Y., Tanikawa, W., Bihan, M., Bowden, S.A., Elvert, M., Glombitza, C., Gross, D., Harrington, G.J., Hori, T., Li, K., Limmer, D., Liu, C.H., Murayama, M., Ohkouchi, N., Ono, S., Park, Y.S., Phillips, S.C., Prieto-Mollar, X., Purkey, M., Riedinger, N., Sanada, Y., Sauvage, J., Snyder, G., Susilawati, R., Takano, Y., Tasumi, E., Terada, T., Tomaru, H., Trembath-Reichert, E., Wang, D.T., and Yamada, Y., 2015. Exploring deep microbial life in coal-bearing sediment down to ~2.5 km below the ocean floor. *Science*, 349(6246):420–424. **https://doi.org/10.1126/science.aaa6882**

Jerram, D.A., Millett, J.M., Kück, J., Thomas, D., Planke, S., Haskins, E., Lautze, N., and Pierdominici, S., 2019. Understanding volcanic facies in the subsurface: a combined core, wireline logging and image log data set from the PTA2 and KMA1 boreholes, Big Island, Hawai'i. *Scientific Drilling*, 25:15–33. **https://doi.org/10.5194/sd-25-15-2019**

Jolley, D.W., Clarke, B., and Kelley, S., 2002. Paleogene time scale miscalibration: evidence from the dating of the North Atlantic igneous province. *Geology*, 30(1):7–10. **https://doi.org/10.1130/0091-7613(2002)030%3C0007:PTSMEF%3E2.0.CO;2**

Jones, M.T., Jerram, D.A., Svensen, H.H., and Grove, C., 2016. The effects of large igneous provinces on the global carbon and sulphur cycles. *Palaeogeography, Palaeoclimatology, Palaeoecology*, 441:4–21. **https://doi.org/10.1016/j.palaeo.2015.06.042**

Kjoberg, S., Schmidedel, T., Planke, S., Svensen, H.H., Millett, J.M., Jerram, D.A., Galland, O., Lecomte, I., Schofield, N., Haug, Ø.T., and Helsem, A., 2017. 3D structure and formation of hydrothermal vent complexes at the Paleocene-Eocene transition, the Møre Basin, mid-Norwegian margin. *Interpretation*, 5(3):1A–T449. **https://doi.org/10.1190/INT-2016-0159.1**

Kuiper, K.F., Deino, A., Hilgen, F.J., Krijgsman, W., Renne, P.R., and Wijbrans, J.R., 2008. Synchronizing rock clocks of Earth history. *Science*, 320(5875):500–504. **https://doi.org/10.1126/science.1154339**

Kusznir, N.J., Hunsdale, R., and Roberts, A.M., 2004. Timing of depth-dependent lithosphere stretching on the S. Lofoten rifted margin offshore mid-Norway: pre-breakup or post-breakup? *Basin Research*, 16(2):279–296. **https://doi.org/10.1111/j.1365-2117.2004.00233.x**

Larsen, H.C., and Saunders, A.D., 1998. Tectonism and volcanism at the southeast Greenland rifted margin; a record of plume impact and later continental rupture. *In* Saunders, A.D., Larsen, H.C. and Wise, S.W.J. (Eds.), *Proceedings of the Ocean Drilling Program, Scientific Results*, 152: College Station, TX (Ocean Drilling Program), 503–533. **https://doi.org/10.2973/odp.proc.sr.152.240.1998**

Larsen, H.C., Saunders, A.D., Clift, P.D., et al., 1994. *Proceedings of the Ocean Drilling Program, Initial Reports,* 152: College Station, TX: Ocean Drilling Program. **https://doi.org/10.2973/odp.proc.ir.152.1994**

Larsen, L.M., Pedersen, A.K., Tegner, C., Duncan, R.A., Hald, N., and Larsen, J.G., 2016. Age of Tertiary volcanic rocks on the west Greenland continental margin: volcanic evolution and event correlation to other parts of the North Atlantic Igneous Province. *Geological Magazine*, 153(3):487–511. **https://doi.org/10.1017/S0016756815000515**

Larsen, L.M., Rex, D.C., Watt, W.S., and Guise, P.G., 1999. $^{40}Ar–^{39}Ar$ dating of alkali basaltic dykes along the southwest coast of Greenland: Cretaceous and Tertiary igneous activity along the eastern margin of the Labrador Sea. *Geology of Greenland Survey Bulletin*, 184:19–29. **https://doi.org/10.34194/ggub.v184.5227**

Littler, K., Röhl, U., Westerhold, T., and Zachos, J.C., 2014. A high-resolution benthic stable-isotope record for the South Atlantic; implications for orbital-scale changes in late Paleocene-early Eocene climate and carbon cycling. *Earth and Planetary Science Letters*, 401:18–30. **https://doi.org/10.1016/j.epsl.2014.05.054**

Lundin, E.R., and Doré, A.G., 2005. NE Atlantic break-up: a re-examination of the Iceland mantle plume model and the Atlantic–Arctic linkage. *Geological Society of London, Petroleum Geology Conference Series*, 6(1):739–754. **https://doi.org/10.1144/0060739**

Mahoney, J.J., and Coffin, M.F., 1997. *Large Igneous Provinces: Continental, Oceanic, and Planetary Flood Volcanism*. Geophysical Monograph, 100. **https://doi.org/10.1029/GM100**

McKenzie, D., and Bickle, M.J., 1988. The volume and composition of melt generated by extension of the lithosphere. *Journal of Petrology*, 29(3):625–679. **https://doi.org/10.1093/petrology/29.3.625**

Millett, J.M., Manton, B.M., Zastrozhnov, D., Planke, S., Maharjan, D., Bellwald, B., Gernigon, L., Faleide, J.I., Jolley, D.W., Walker, F., Abdelmalak, M.M., Jerram, D.A., Myklebust, R., Kjølhamar, B.E., Halliday, J., and Birch-Hawkins, A., 2020. Basin structure and prospectivity of the NE Atlantic volcanic rifted margin: cross-border examples from the Faroe–Shetland, Møre and Southern Vøring Basins. *Geological Society Special Publication*, 495:SP495-2019-2012. **https://doi.org/10.1144/sp495-2019-12**

Mjelde, R., Raum, T., Breivik, A., Shimamura, H., Murai, Y., Takanami, T., and Faleide, J.I., 2005. Crustal structure of the Vøring Margin, NE Atlantic: a review of geological implications based on recent OBS data. *Geological Society of London, Petroleum Geology Conference Series*, 6(1):803–813. **https://doi.org/10.1144/0060803**

Mutter, J.C., Buck, W.R., and Zehnder, C.M., 1988. Convective partial melting: 1. A model for the formation of thick basaltic sequences during the initiation of spreading. *Journal of Geophysical Research: Solid Earth*, 93(B2):1031–1048. **https://doi.org/10.1029/JB093iB02p01031**

Ogg, J.G., 2012. Geomagnetic Polarity Time Scale. *In* Gradstein, F.M., Ogg, J.G., Schmitz, M.D. and Ogg, G.M. (Eds.), *The Geologic Time Scale*: Boston (Elsevier), 85–113. **https://doi.org/10.1016/B978-0-444-59425-9.00005-6**

Pagani, M., Pedentchouk, N., Huber, M., Sluijs, A., Schouten, S., Brinkhuis, H., Sinninghe Damsté, J.S., Dickens, G.R., Backman, J., Clemens, S., Cronin, T., Eynaud, F., Gattacceca, J., Jakobsson, M., Jordan, R., Kaminski, M., King, J., Koc, N., Martinez, N.C., McInroy, D., Moore Jr, T.C., O'Regan, M., Onodera, J., Pälike, H., Rea, B., Rio, D., Sakamoto, T., Smith, D.C., St John, K.E.K., Suto, I., Suzuki, N., Takahashi, K., Watanabe, M., Yamamoto, M., and Expedition Scientists, 2006. Arctic hydrology during global warming at the Palaeocene/Eocene Thermal Maximum. *Nature*, 442(7103):671–675. **https://doi.org/10.1038/nature05043**

Parnell-Turner, R., Cann, J.R., Smith, D.K., Schouten, H., Yoerger, D., Palmiotto, C., Zheleznov, A., and Bai, H., 2014. Sedimentation rates test models of oceanic detachment faulting. *Geophysical Research Letters*, 41(20):7080–7088. **https://doi.org/10.1002/2014GL061555**

Planke, S., 1994. Geophysical response of flood basalts from analysis of wire line logs; Ocean Drilling Program Site 642, Vøring volcanic margin. *Journal of Geophysical Research: Solid Earth*, 99(B5):9279–9296. **https://doi.org/10.1029/94JB00496**

Planke, S., Millett, J.M., Maharjan, D., Jerram, D.A., Abdelmalak, M.M., Groth, A., Hoffmann, J., Berndt, C., and Myklebust, R., 2017. Igneous seismic geomorphology of buried lava fields and coastal escarpments on the Vøring volcanic rifted margin. *Interpretation*, 5(3):SK161–SK177. **https://doi.org/10.1190/INT-2016-0164.1**

Planke, S., Rasmussen, T., Rey, S.S., and Myklebust, R., 2005. Seismic characteristics and distribution of volcanic intrusions and hydrothermal vent complexes in the Vøring and Møre Basins. *Geological Society of London, Petroleum Geology Conference Series*, 6(1):833–844. **https://doi.org/10.1144/0060833**

Planke, S., Symonds, P.A., Alvestad, E., and Skogseid, J., 2000. Seismic volcanostratigraphy of large-volume basaltic extrusive complexes on rifted margins. *Journal of Geophysical Research: Solid Earth*, 105(B8):19335–19351. **https://doi.org/10.1029/1999JB900005**

Polteau, S., Planke, S., Zastrozhnov, D., Abdelmalak, M.M., Lebedeva-Ivanova, N., Planke, E.E., Svensen, H.H., Mazzini, A., Gernigon, L., Myklebust, R., Kjølhamar, B.E., Pedersen, R.B., Sandstå, N.R., and Bünz, S., 2020. Upper Cretaceous-Paleogene stratigraphy and development of the Mímir high, Vøring transform margin, Norwegian Sea. *Marine and Petroleum Geology*, 122:104717. **https://doi.org/10.1016/j.marpetgeo.2020.104717**

Reynolds, P., Planke, S., Millett, J.M., Jerram, D.A., Trulsvik, M., Schofield, N., and Myklebust, R., 2017. Hydrothermal vent complexes offshore northeast Greenland: a potential role in driving the PETM. *Earth and Planetary Science Letters*, 467:72–78. **https://doi.org/10.1016/j.epsl.2017.03.031**

Ritchie, J.D., Gatliff, R.W., and Richards, P.C., 1999. Early Tertiary magmatism in the offshore NW UK margin and surrounds. *Geological Society of London, Petroleum Geology Conference Series*, 5(1):573–584. **https://doi.org/10.1144/0050573**

Sanei, H., Grasby, S.E., and Beauchamp, B., 2012. Latest Permian mercury anomalies.*Geology*, 40(1):63–66. **https://doi.org/10.1130/G32596.1**

Saunders, A.D., Jones, S.M., Morgan, L.A., Pierce, K.L., Widdowson, M., and Xu, Y.G., 2007. Regional uplift associated with continental large igneous provinces: the roles of mantle plumes and the lithosphere. *Chemical Geology*, 241(3–4):282–318. **https://doi.org/10.1016/j.chemgeo.2007.01.017**

Saunders, A.D., Larsen, H.C., and Fitton, J.G., 1998. Magmatic development of the Southeast Greenland margin and evolution of the Iceland plume; geochemical constraints from Leg 152. *In* Saunders, A.D., Larsen, H.C. and Wise, S.W., Jr. (Eds.), *Proceedings of the Ocean Drilling Program, Scientific Results*, 152: College Station, TX (Ocean Drilling Program), 479–501. **https://doi.org/10.2973/odp.proc.sr.152.239.1998**

Sengör, A.M.C., and Burke, K., 1978. Relative timing of rifting and volcanism on Earth and its tectonic implications. *Geophysical Research Letters*, 5(6):419–421. **https://doi.org/10.1029/GL005i006p00419**

Skogseid, J., Planke, S., Faleide, J.I., Pedersen, T., Eldholm, O., and Neverdal, F., 2000. NE Atlantic continental rifting and volcanic margin formation. *Geological Society Special Publication*, 167(1):295–326. **https://doi.org/10.1144/GSL.SP.2000.167.01.12**

Storey, M., Duncan, R.A., Pedersen, A.K., Larsen, L.M., and Larsen, H.C., 1998. $^{40}Ar/^{39}Ar$ geochronology of the west Greenland Tertiary volcanic province. *Earth and Planetary Science Letters*, 160(3):569–586. **https://doi.org/10.1016/S0012-821X(98)00112-5**

Storey, M., Duncan, R.A., and Swisher, C.C., III, 2007a. Paleocene-Eocene Thermal Maximum and the opening of the Northeast Atlantic. *Science*, 316(5824):587–589. **https://doi.org/10.1126/science.1135274**

Storey, M., Duncan, R.A., and Tegner, C., 2007b. Timing and duration of volcanism in the North Atlantic Igneous Province: implications for geodynamics and links to the Iceland hotspot. *Chemical Geology*, 241(3):264–281. **https://doi.org/10.1016/j.chemgeo.2007.01.016**

Suan, G., Popescu, S.-M., Suc, J.-P., Schnyder, J., Fauquette, S., Baudin, F., Yoon, D., Piepjohn, K., Sobolev, N.N., and Labrousse, L., 2017. Subtropical climate conditions and mangrove growth in Arctic Siberia during the early Eocene. *Geology*, 45(6):539–542. **https://doi.org/10.1130/G38547.1**

Svensen, H., Planke, S., and Corfu, F., 2010. Zircon dating ties NE Atlantic sill emplacement to initial Eocene global warming. *Journal of the Geological Society*, 167(3):433–436. **https://doi.org/10.1144/0016-76492009-125**

Svensen, H., Planke, S., Malthe-Sørenssen, A., Jamtveit, B., Myklebust, R., Rasmussen Eidem, T., and Rey, S.S., 2004. Release of methane from a volcanic basin as a mechanism for initial Eocene global warming. *Nature*, 429(6991):542–545. **https://doi.org/10.1038/nature02566**

Talwani, M., and Eldholm, O., 1977. Evolution of the Norwegian-Greenland Sea. *Geological Society of America Bulletin*, 88(7):969–999. **https://doi.org/10.1130/0016-7606(1977)88%3C969:EOTNS%3E2.0.CO;2**

Tegner, C., Lesher, C.E., Larsen, L.M., and Watt, W.S., 1998. Evidence from the rare-earth-element record of mantle melting for cooling of the Tertiary Iceland plume. *Nature*, 395(6702):591–594. **https://doi.org/10.1038/26956**

Theissen-Krah, S., Zastrozhnov, D., Abdelmalak, M.M., Schmid, D.W., Faleide, J.I., and Gernigon, L., 2017. Tectonic evolution and extension at the Møre margin – offshore mid-Norway. *Tectonophysics*, 721:227–238. **https://doi.org/10.1016/j.tecto.2017.09.009**

Vogt, P.R., 1972. Evidence for global synchronism in mantle plume convection, and possible significance for geology. *Nature*, 240(5380):338–342. **https://doi.org/10.1038/240338a0**

Westerhold, T., Marwan, N., Drury, A.J., Liebrand, D., Agnini, C., Anagnostou, E., Barnet, J.S.K., et al., 2020. An astronomically dated record of Earth's climate and its predictability over the last 66 million years. *Science*, 369(6509):1383–1387. **https://doi.org/10.1126/science.aba6853**

White, R., and McKenzie, D., 1989. Magmatism at rift zones: the generation of volcanic continental margins and flood basalts. *Journal of Geophysical Research: Solid Earth*, 94(B6):7685–7729. **https://doi.org/10.1029/JB094iB06p07685**

Wignall, P.B., 2001. Large igneous provinces and mass extinctions. *Earth-Science Reviews*, 53(1):1–33. **https://doi.org/10.1016/S0012-8252(00)00037-4**

Wilkinson, C.M., Ganerød, M., Hendriks, B.W.H., and Eide, E.A., 2017. Compilation and appraisal of geochronological data from the North Atlantic Igneous Province (NAIP). *Geological Society Special Publication*, 447(1):69–103. **https://doi.org/10.1144/sp447.10**

Wright, K.A., Davies, R.J., Jerram, D.A., Morris, J., and Fletcher, R., 2012. Application of seismic and sequence stratigraphic concepts to a lava-fed delta system in the Faroe-Shetland Basin, UK and Faroes. *Basin Research*, 24(1):91–106. **https://doi.org/10.1111/j.1365-2117.2011.00513.x**

Zastrozhnov, D., Gernigon, L., Gogin, I., Abdelmalak, M.M., Planke, S., Faleide, J.I., Eide, S., and Myklebust, R., 2018. Cretaceous-Paleocene evolution and crustal structure of the northern Vøring margin (offshore mid-Norway): results from integrated geological and geophysical study. *Tectonics*, 37(2):497–528. **https://doi.org/10.1002/2017TC004655**

Zastrozhnov, D., Gernigon, L., Gogin, I., Planke, S., Abdelmalak, M.M., Polteau, S., Faleide, J.I., Manton, B., and Myklebust, R., 2020. Regional structure and polyphased Cretaceous-Paleocene rift and basin development of the mid-Norwegian volcanic passive margin. *Marine and Petroleum Geology*, 115:104269. **https://doi.org/10.1016/j.marpetgeo.2020.104269**

Ziegler, P.A., and Cloetingh, S., 2004. Dynamic processes controlling evolution of rifted basins. *Earth-Science Reviews*, 64(1):1–50. **https://doi.org/10.1016/S0012-8252(03)00041-2**

Table T1. Summary of primary sites and drilling targets, Expedition 396. Sites were located based on seismic data in ED50/UTM31 and then transformed to WGS84 latitude/longitude. SP = shotpoint, HR = high resolution, APC = advanced piston corer, XCB = extended core barrel, RCB = rotary core barrel, VSP = vertical seismic profile, UBI = Ultrasonic Borehole Imager, HTVC = hydrothermal vent complex, PETM = Paleocene/Eocene Thermal Maximum, SDR = seaward-dipping reflector.

https://doi.org/10.14379/iodp.sp.396.2021

Site name	Primary/ Alternate	Longitude (WGS84)	Latitude (WGS84)	UTM31 (X) WGS84	UTM31 (Y) WGS84	Longitude (ED50)	Latitude (ED50)	UTM31 (X) ED50	UTM31 (Y) ED50	Seismic volume	In-line number	SP-Primary Line	Cross-line	SP-Crossing Line	Main line (HR)	Cross-line (HR)	Main line (CAGE20-4)	Cross-line (CAGE20-4)	Water depth (m)	Sediments	Basalt thickness (m)	Total depth (m)	Target	Location	High priority	Drilling order	Sub-pri	APC/ XCB	RCB	Duplicate	VSP	Logs	UBI	Comments
VMVM-20A	Pri	2.74982	64.96270	488186	7204320	2.75180	64.96300	488279	7204530	AMN17-PRCMIG	6464	1020	1294	6464	AMN17-PRCMIG-6464	AMN17-PRCMIG-1294	2D Line 002	2D Line 005 and 001	2077	30 m Neogene	0	200	Sub-basalt	Kolga High		1	1		x			x	(x)	
VMVM-21A	Alt	2.74682	64.95750	488042	7203740	2.74880	64.95780	488135	7203960	AMN17-PRCMIG	6496	1020	1294	6496	AMN17-PRCMIG-6496	AMN17-PRCMIG-1294	2D Line 003	2D Line 005	2078	45 m Neogene	0	200	Sub-basalt	Kolga High			2		x			x	(x)	
VMVM-22A	Alt	2.78692	64.94460	489931	7202290	2.78890	64.94490	490024	7202510	AMN17-PRCMIG	6547	1194	1468	6547	AMN17-PRCMIG-6547	AMN17-PRCMIG-1468	2D Line 004	—	2017	85 m Neogene	0	200	Sub-basalt	Kolga High			3		x			x	(x)	
VMVM-23A	Pri	2.72922	64.96480	487214	7204550	2.73120	64.96510	487307	7204770	AMN17-PRCMIG	6464	940	1214	6464	AMN17-PRCMIG-6464	AMN17-PRCMIG-1214	2D Line 002	2D Line 006 and 007	2137	25 m Neogene	375	400	Initial basalt	Kolga High		2	1		x		(x)	(x)	(x)	
VMVM-24A	Alt	2.72622	64.95960	487070	7203980	2.72820	64.95990	487163	7204190	AMN17-PRCMIG	6496	940	1214	6496	AMN17-PRCMIG-6496	AMN17-PRCMIG-1214	2D Line 003	2D Line 006	2145	30 m Neogene	370	400	Initial basalt	Kolga High			2		x		(x)	(x)	(x)	
VMVM-25A	Alt	2.72152	64.95120	486844	7203040	2.72350	64.95150	486937	7203260	AMN17-PRCMIG	6547	940	1214	6547	AMN17-PRCMIG-6547	AMN17-PRCMIG-1214	2D Line 004	2D Line 006	2160	25 m Neogene	375	400	Initial basalt	Kolga High			3		x		(x)	(x)	(x)	
VMVM-31A	Pri	3.05430	65.36420	502526	7249040	3.05630	65.36450	502619	7249260	AMN17-PRCMIG	3966	1291	1565	3966	AMN17-PRCMIG-3966	AMN17-PRCMIG-1565	HydroVent3D	HydroVent3D, 2D Line 008	1707	55 m pre-Paleocene	0	200	Paleogene sediments	North Modgunn		3	1		(x)			x		
VMVM-32A	Alt	3.05850	65.37140	502720	7249850	3.06050	65.37170	502813	7250060	AMN17-PRCMIG	3922	1291	1565	3922	AMN17-PRCMIG-3922	AMN17-PRCMIG-1565	HydroVent3D	HydroVent3D, 2D Line 008	1695	55 m pre-Paleocene	0	200	Paleogene sediments	North Modgunn			2		(x)			x		
VMVM-33A	Alt	3.09269	65.40620	504305	7253730	3.09470	65.40650	504398	7253950	AMN17-PRCMIG	3701	1341	1615	3701	AMN17-PRCMIG-3701	AMN17-PRCMIG-1615	2D Line 009	2D Line 010	1673	110 m pre-Paleocene	0	200	Paleogene sediments	North Modgunn			3		(x)			x		
VMVM-40B	Pri	3.05180	65.35990	502410	7248560	3.05380	65.36020	502503	7248780	AMN17-PRCMIG	3992	1291	1565	3992	AMN17-PRCMIG-3992	AMN17-PRCMIG-1565	HydroVent3D	HydroVent3D, 2D Line 008	1696	40 m pre-Paleocene	0	200	HTVC	North Modgunn	X	4	1							Gas, mineralization
VMVM-41A	Alt	3.06120	65.37590	502845	7250350	3.06320	65.37620	502938	7250570	AMN17-PRCMIG	3894	1291	1565	3894	AMN17-PRCMIG-3894	AMN17-PRCMIG-1565	HydroVent3D	HydroVent3D, 2D Line 008	1686	65 m pre-Paleocene	0	200	HTVC	North Modgunn			2							Gas, mineralization
VMVM-42A	Alt	3.07149	65.40830	503320	7253960	3.07350	65.40860	503413	7254180	AMN17-PRCMIG	3701	1260	1534	3701	AMN17-PRCMIG-3701	AMN17-PRCMIG-1534	CAGE20-4, 2D Line 009	—	1695	135 m pre-Paleocene	0	300	HTVC	North Modgunn			3							Gas, mineralization
VMVM-51A	Alt	1.95852	65.87320	452498	7306170	1.96060	65.87350	452591	7306390	CFI-MNR J-Cube MN	CFI-MNR11-7324	7178	14213	24851	— —	— —	2D Line 017	2D Line 018	2147	200 m pre-Paleocene	0	800	Mimir High	Mimir High			2	x	x	x	x	x		Duplicate on PETM (if we find it)
VMVM-55B	Pri	2.02682	65.83130	455541	7301450	2.02890	65.83160	455634	7301670	CFI-MNR	CFI-MNR07-7319	15560			—	—	MimirHigh3D, 2D Line 017	MimirHigh3D, 2D Line 013	2186	255 m pre-Paleocene	0	800	Mimir High	Mimir High	X	5	1	x	x	x	x	x		Duplicate on PETM (if we find it)
VMVM-56A; Start | Ribbon	Alt	1.95602	65.82800	452300	7301130	1.95810	65.82830	452393	7301350	CFI-MNR	CFI-MNR07-7319	15300			—	—	MimirHigh3D	MimirHigh3D, 2D Line 013	2285		0	200	Mimir High	Mimir High			3	x	x	x		x		Duplicate on PETM (if we find it)
VMVM-56A; End | Ribbon	Alt	1.99962	65.83010	454296	7301330	2.00170	65.83040	454389	7301550	CFI-MNR	CFI-MNR07-7319	15460			—	—	MimirHigh3D	MimirHigh3D, 2D Line 013	2203		0	200	Mimir High	Mimir High			3	x	x	x		x		Duplicate on PETM (if we find it)
VMVM-61A	Pri	3.73746	67.30670	531749	7465760	3.73960	67.30690	531842	7465980	CVX1101-PSTM	1852	3267	5057	1062	—	—	—	—	1200	125 m	175	300	Basalt sequence 1	Skoll High	X	6	1		x		x	x	x	
VMVM-62A	Alt	3.67576	67.28910	529114	7463760	3.67790	67.28930	529208	7463980	CVX1101-PSTM	1832	3006	4796	1042	—	—	—	—	1198	115 m	185	300	Basalt sequence 2	Skoll High			2		x		x	x	x	
VMVM-07A	Pri	3.61935	67.33080	526638	7468390	3.62150	67.33100	526731	7468610	CVX1101-PSTM	2041	2436	4796	1251	—	—	—	—	1206	220 m	180	400	Basalt sequence 2	Skoll High	X	7	1		x		x	x	x	Intra basalt sediments
VMVM-71A	Alt	3.69456	67.33840	529862	7469270	3.69670	67.33860	529956	7469490	CVX1101-PSTM	2012	3267	5057	1222	—	—	—	—	1200	195 m	205	400	Basalt sequence 3	Skoll High			2		x		x	x	x	Intra basalt sediments
VMVM-80A	Pri	4.64057	68.60020	566797	7610680	4.64280	68.60040	566890	7610900	HV96	HV96-7	4728			—	—	—	—	2864	210 m	100	310	Outer High	Norwegian Sea		8	1						x	Intra basalt sediments
VMVM-81A	Alt	4.58257	68.62640	564360	7613540	4.58480	68.62660	564454	7613760	HV96	HV96-7	5030			—	—	—	—	2913	55 m	145	200	Outer High	Norwegian Sea			2						x	Intra basalt sediments
VMVM-09A	Pri	5.79491	68.76040	612963	7630210	5.79710	68.76050	613057	7630430	HV96	HV96-6	2355			—	—	—	—	3156	450 m	100	550	Outer SDR	Norwegian Sea		9	1	x	x		x	x	(x)	
VMVM-10B	Alt	4.12833	68.83040	545472	7635870	4.13060	68.83060	545565	7636090	HV96	HV96-7	7370	HV96-8	495	—	—	—	—	3237	650 m	100	750	Outer SDR	Norwegian Sea			2	x	x		x	x	(x)	

Table T2. Operations and time estimate for primary sites, Expedition 396. Site coordinates in WGS84. EPSP = Environmental Protection and Safety Panel, RCB = rotary core barrel, APC = advanced piston corer, XCB = extended core barrel, triple combo = triple combination, UBI = Ultrasonic Borehole Imager, FMS = Formation MicroScanner, VSP = vertical seismic profile.

Site No.	Location (Latitude Longitude)	Seafloor Depth (mbrf)	Operations Description	Transit (days)	Drilling Coring (days)	Logging (days)
Reykjavik			Begin Expedition 5.0	port call days		
			Transit ~735 nmi to VMVM-20A @ 10.5	2.9		
VMVM-20A	64° 57.7620' N	2088	Hole A - RCB to 200 mbsf - Log with Triple Combo w/UBI & FMS Sonic		2.0	0.8
EPSP	2° 44.9892' E					
to 200 mbsf						
			Sub-Total Days On-Site: 2.8			
			Transit ~1 nmi to VMVM-23A @ 1.5	0.0		
VMVM-23A	64° 57.8880' N	2148	Hole A - RCB to 200 mbsf - Log with Triple Combo w/UBI, FMS Sonic & VSP		4.3	0.9
EPSP	2° 43.7532' E					
to 400 mbsf						
			Sub-Total Days On-Site: 5.2			
			Transit ~25 nmi to VMVM-31A @ 10.5	0.1		
VMVM-31A	65° 21.8520' N	1718	Hole A - APC/XCB to 200 mbsf - Log with Triple Combo w/UBI, FMS Sonic & VSP		1.5	0.7
EPSP	3° 3.2580' E					
to 200 mbsf						
			Sub-Total Days On-Site: 2.2			
			Transit ~0 nmi to VMVM-40B @ 1.5	0.0		
VMVM-40B	65° 21.5940' N	1707	Hole A - XCB to 200 mbsf		1.5	
EPSP	3° 3.1080' E		Hole B - XCB to 200 mbsf - Log with Triple Combo, FMS Sonic & VSP		1.5	0.7
to 200 mbsf						
			Sub-Total Days On-Site: 3.7			
			Transit ~38 nmi to VMVM-55B @ 10.5	0.1		
VMVM-55B	65° 49.8780' N	2197	Hole A - XCB to 300 mbsf		2.1	
EPSP	2° 1.6092' E		Hole B - RCB to 800 mbsf - Log with Triple Combo, FMS Sonic & VSP		6.9	1.9
to 800 mbsf						
			Sub-Total Days On-Site: 10.9			
			Transit ~97 nmi to VMVM-61A @ 10.5	0.4		
VMVM-61A	67° 18.4020' N	1211	Hole A - RCB to 240 mbsf - Log with Triple Combo w/UBI, FMS Sonic & VSP		3.1	0.9
EPSP	3° 44.2476' E					
to 300 mbsf						
			Sub-Total Days On-Site: 4.0			
			Transit ~3 nmi to VMVM-07A @ 1.5	0.1		
VMVM-07A	67° 19.8480' N	1217	Hole A - RCB to 320 mbsf - Log with Triple Combo w/UBI, FMS Sonic & VSP		3.6	1.0
EPSP	3° 37.1610' E					
to 400 mbsf						
			Sub-Total Days On-Site: 4.6			
			Transit ~80 nmi to VMVM-80A @ 10.5	0.3		
VMVM-80A	68° 36.0120' N	2875	Hole A - RCB to 310 mbsf - Log with Triple Combo w/UBI & FMS Sonic		4.2	0.9
EPSP	4° 38.4342' E					
to 310 mbsf						
			Sub-Total Days On-Site: 4.6			
			Transit ~27 nmi to VMVM-09A @ 10.5	0.1		
VMVM-09A	68° 45.6240' N	3167	Hole A - RCB to 550 mbsf - Log with Triple Combo w/UBI, FMS Sonic & VSP		6.9	1.5
EPSP	5° 47.6940' E		Hole B - APC/XCB to 200 mbsf		2.1	
to 550 mbsf						
			Sub-Total Days On-Site: 10.5			
			Transit ~764 nmi to Kristiansand @ 10.5	3.0		
Kristiansand			End Expedition	7.0	39.7	9.3

Port Call:	5.0	Total Operating Days:	56.0
Sub-Total On-Site:	49.0	Total Expedition:	61.0

Figure F1. Distribution of Paleogene igneous breakup complexes and oceanic structures in northeast and northwest Atlantic. Scientific boreholes and proposed drilling sites are shown. Compiled from Abdelmalak et al. (2016a, 2016b, 2017, 2019), Berndt et al. (2001b), Boldreel and Andersen (1994), Davison et al. (2010), Elliott and Parson (2008), Geissler et al. (2016), Reynolds et al. (2017), and Ritchie et al. (1999). SDR = seaward-dipping reflector.

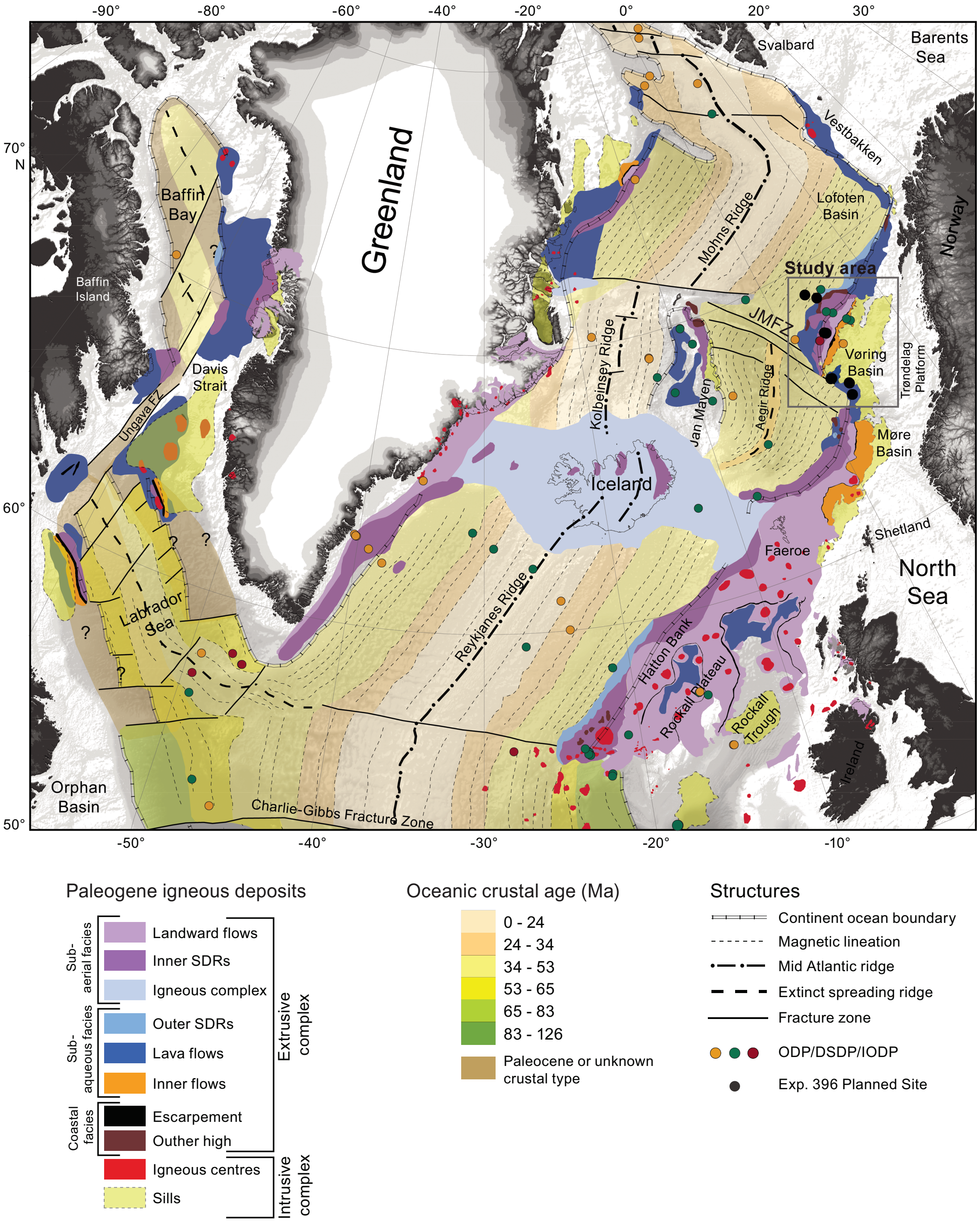

Figure F2. Schematic crustal profile across central part of mid-Norwegian continental (cont.) margin, focusing on volcanic seismic facies units (italics; see Planke et al., 2000) and intrusive magmatic complexes. Modified from Millett et al. (2020), Zastrozhnov et al. (2020), and Abdelmalak et al. (2017). SDR = seaward-dipping reflector, COB = continent/ocean boundary, LCB = lower crustal body, TR = T-reflection, sed. = sediments.

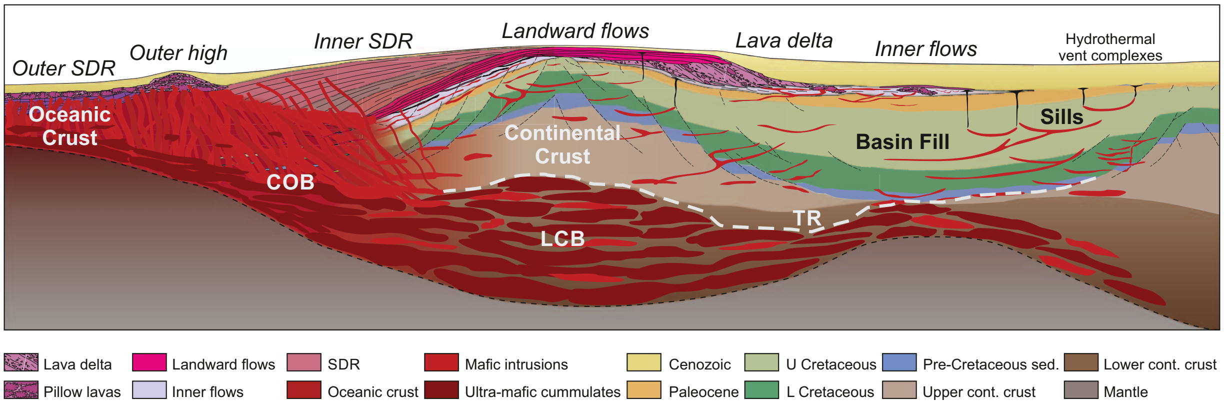

Figure F3. Melt generation models of volcanic rifted margins. A. Igneous oceanic crustal thickness vs. spreading rate (Bown and White, 1994). B. Contrasting rifted margin magmatic modes. C. Forward model prediction of "normal" magmatic margin with 6 km igneous crust. D. Model prediction of igneous crustal thickness as a function of mantle potential temperature (G. Lu and R. Huismans, pers. comm., 2020). COB = continent/ocean boundary, MOR = mid-ocean ridge.

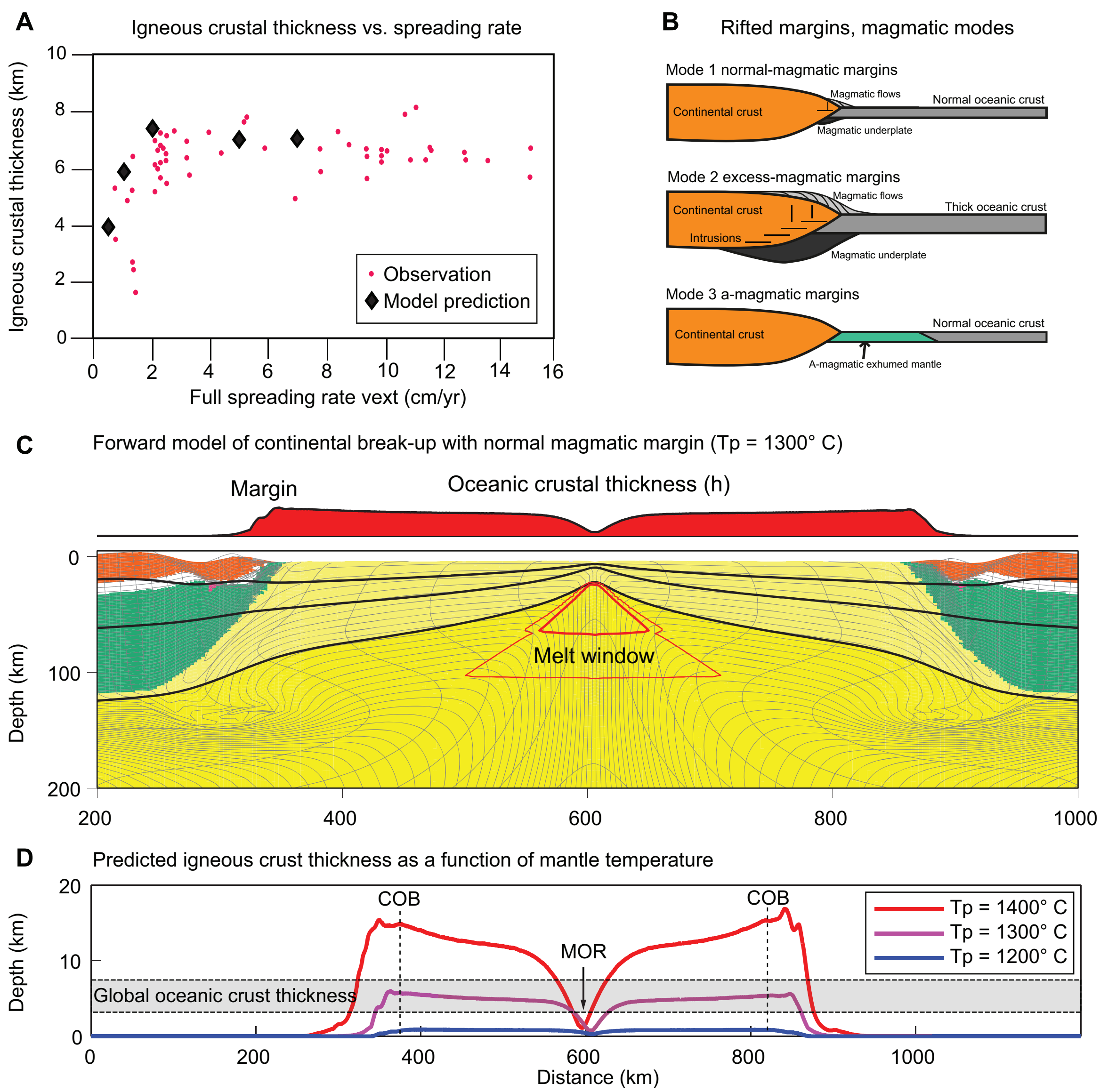

Figure F4. Data base and structural framework of the mid-Norwegian volcanic rifted margin (study area in Figure F1; modified from Zastrozhnov et al., 2020). Light gray dots = Expedition 396 primary proposed sites. Data courtesy of TGS. SDR = seaward-dipping reflector, HTVC = hydrothermal vent complex.

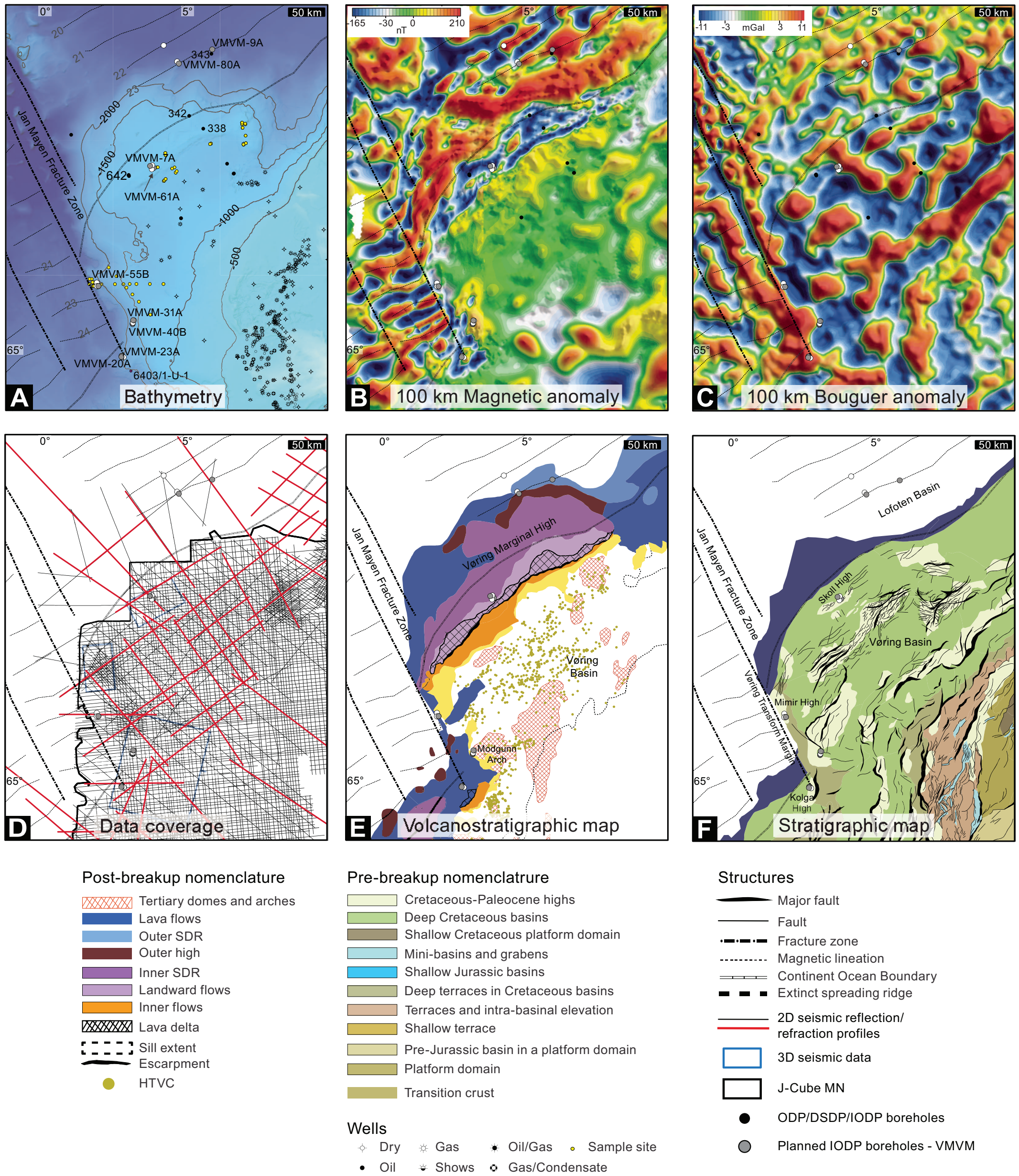

Figure F5. Interpreted basalt distribution and geomorphology along mid-Norwegian volcanic rifted margin (study area in Figure F1; modified from Millett et al., 2020). A–C. Data courtesy of TGS. A, B. Basalt distribution and thickness on north Møre and Vøring margins based on extensive seismic mapping of regional 2-D and recent industry 3-D seismic cubes. C. Thickness of postbreakup sediments showing regions with sediment thickness <200 m in color scale. D. Part of seismic 3-D cube on Vøring Marginal High showing location of Proposed Sites VMVM-61A and VMVM-07A. Site VMVM-61A will sample lava flow field of Sequence 2. Site VMVM-07A will sample onlapping pitted surface of Sequence 1.

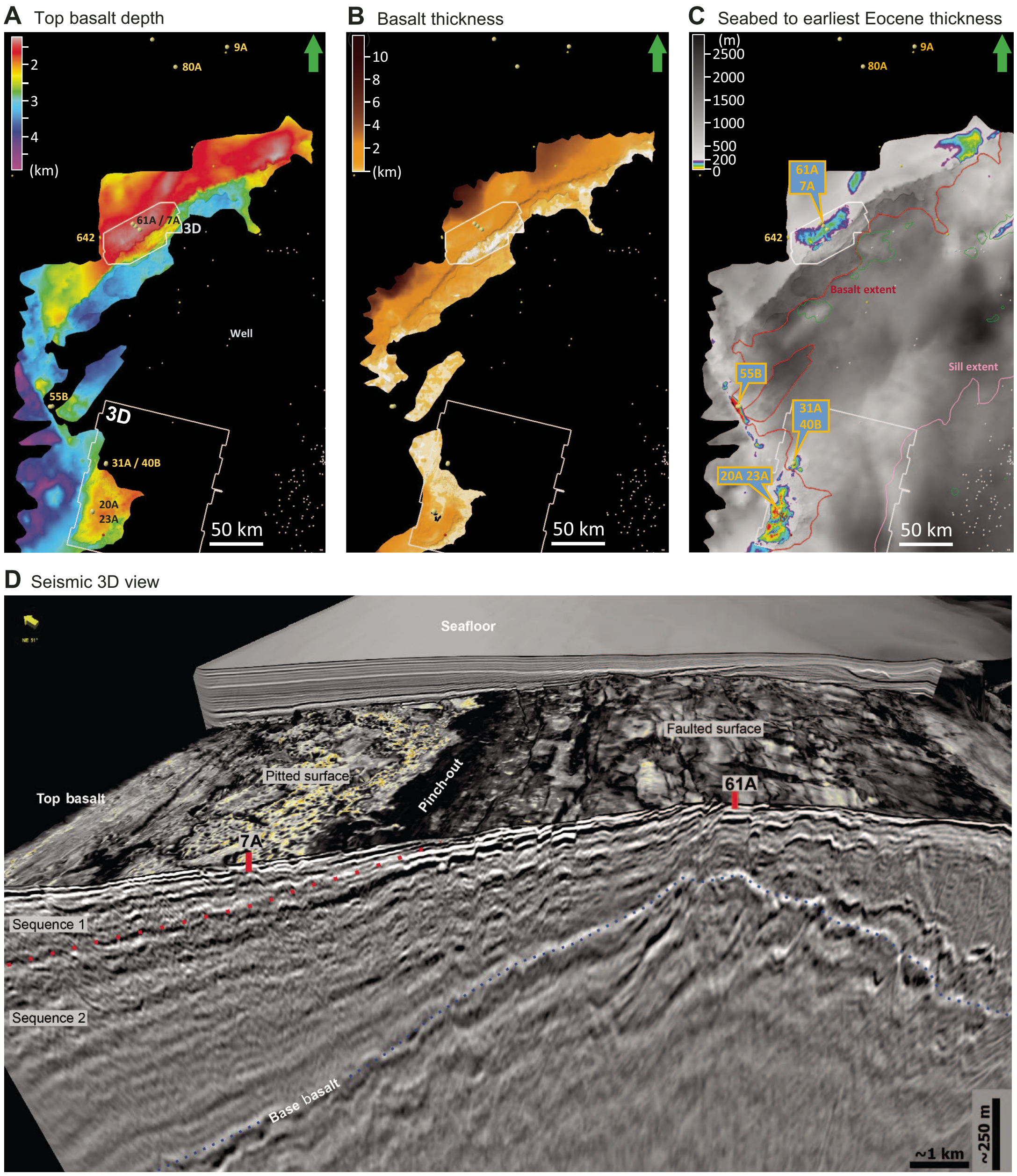

Figure F6. Northeast Atlantic volcanism corresponding to a warming Paleocene–Eocene climate (61.6–50 Ma; green rectangles). Early Paleogene is on 2012 geologic timescale (Ogg, 2012). Age data are filtered to only include robust $^{40}Ar/^{39}Ar$ mineral ages (recalculated to conform to Fish Canyon sanidine age of Kuiper et al., 2008) and U-Pb zircon ID-TIMS ages (Chambers et al., 2005; Ganerød et al., 2010, 2011; Hamilton et al., 1998; Jolley et al., 2002; Larsen et al., 2016; Storey et al., 1998, 2007b; Svensen et al., 2010; Wilkinson et al., 2017). A. Synthesis of climatic proxies (C and O isotopes from Cramer et al. [2009] and Littler et al. [2014]) and known ages of activity in North Atlantic Igneous Province (NAIP). K = Cretaceous. EECO = Early Eocene Climatic Optimum, ETM2 = Eocene Thermal Maximum 2, PETM = Paleocene/Eocene Thermal Maximum. B. Expedition 396 target Paleogene sedimentary interval showing magnetic reversals (magnetochrons), key taxa, palynozones (Kjoberg et al., 2017), and formation names in Vøring Basin. LO = last occurrence. C. Climatic variability of Cenozoic as compiled by Westerhold et al. (2020).

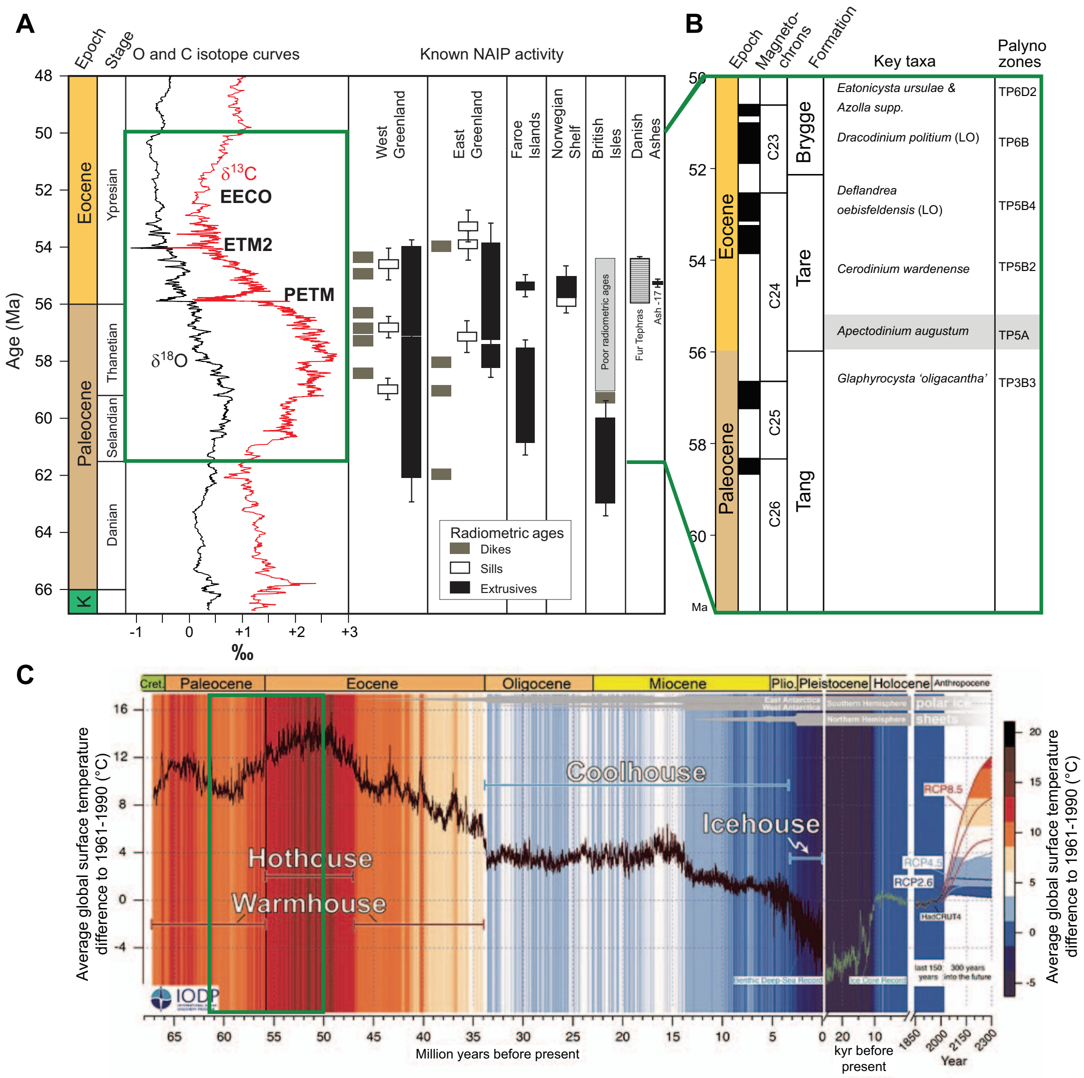

Figure F7. Volcanic seismic facies unit sketch showing schematic location of proposed drill sites (see Figure F2) and seismic reflection data across proposed primary sites. Data courtesy of TGS.

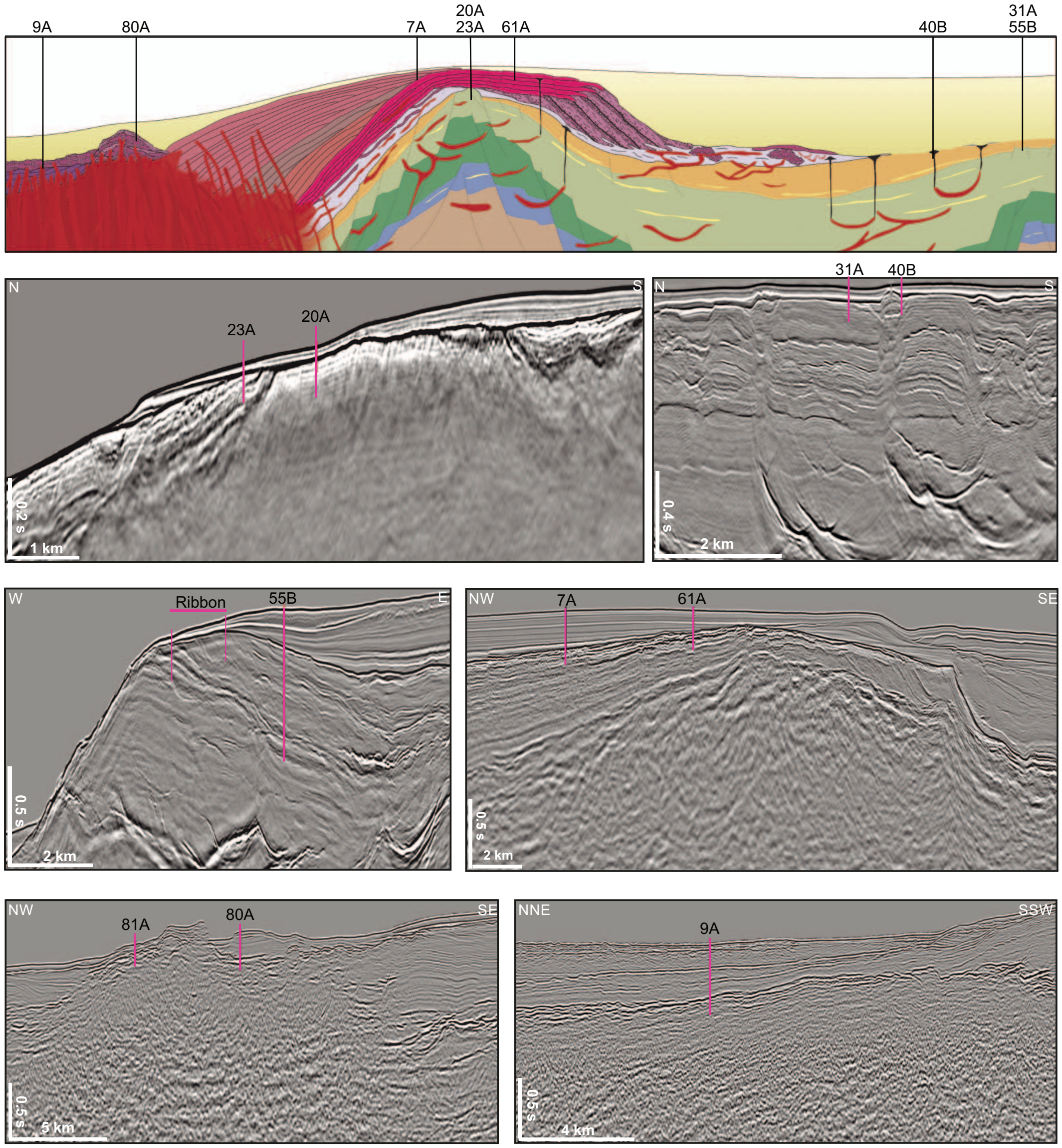

Site summaries

Site VMVM-20A (Kolga High subbasalt)

Priority:	Primary
Position:	64.9627°N, 2.74982°E (WGS84); 64.9630°N, 2.75180°E (ED50)
Water depth (m):	2077
Target drilling depth (mbsf):	200
Approved maximum penetration (mbsf):	200
Survey coverage (track map; seismic profile):	AMN17 (In-line [IL] 6464 shotpoint [SP] 1020/Cross-line [XL] 1294 SP 6464) Track map (Figure **AF1**) Seismic profiles (Figure **AF1**)
Objective(s):	To characterize age and lithology of subbasalt sequences on the Kolga High
Coring program:	Hole A: RCB to bit destruction or 200 mbsf
Downhole measurements program:	Triple combo and FMS-sonic
Nature of rock anticipated:	Pliocene–Pleistocene mud (30 m) above Mesozoic sediments

Site VMVM-21A (Kolga High subbasalt)

Priority:	Alternate
Position:	64.9575°N, 2.74682°E (WGS84); 64.9578°N, 2.74880°E (ED50)
Water depth (m):	2078
Target drilling depth (mbsf):	200
Approved maximum penetration (mbsf):	200
Survey coverage (track map; seismic profile):	AMN17 (IL 6496 SP 1020/XL 1294 SP 6496) Track map (Figure **AF2**) Seismic profiles (Figure **AF2**)
Objective(s):	To characterize age and lithology of subbasalt sequences on the Kolga High
Coring program:	Hole A: RCB to bit destruction or 200 mbsf
Downhole measurements program:	Triple combo and FMS-sonic
Nature of rock anticipated:	Pliocene–Pleistocene mud (45 m) above Mesozoic sediments

Site VMVM-22A (Kolga High subbasalt)

Priority:	Alternate
Position:	64.9446°N, 2.78692°E (WGS84); 64.9449°N, 2.78890°E (ED50)
Water depth (m):	2017
Target drilling depth (mbsf):	200
Approved maximum penetration (mbsf):	200
Survey coverage (track map; seismic profile):	AMN17 (IL 6547 SP 1194/XL 1468 SP 6547) Track map (Figure **AF3**) Seismic profiles (Figure **AF3**)
Objective(s):	To characterize age and lithology of subbasalt sequences on the Kolga High
Coring program:	Hole A: RCB to bit destruction or 200 mbsf
Downhole measurements program:	Triple combo and FMS-sonic
Nature of rock anticipated:	Neogene sediments (85 m)

Site VMVM-23A (Kolga High initial basalt)

Priority:	Primary
Position:	64.9648°N, 2.72922°E (WGS84); 64.9651°N, 2.73120°E (ED50)
Water depth (m):	2137
Target drilling depth (mbsf):	400
Approved maximum penetration (mbsf):	400
Survey coverage (track map; seismic profile):	AMN17 (IL 6464 SP 940/XL 1214 SP 6464) Track map (Figure **AF4**) Seismic profiles (Figure **AF4**)
Objective(s):	To characterize age and lithology of initial basalt sequences on the Kolga High
Coring program:	Hole A: RCB to bit destruction or 400 mbsf
Downhole measurements program:	Triple combo, FMS-sonic-UBI, and vertical seismic profile (VSP)
Nature of rock anticipated:	Pliocene–Pleistocene mud (25 m) above Paleogene lava flows

Site VMVM-24A (Kolga High initial basalt)

Priority:	Alternate
Position:	64.9596°N, 2.72622°E (WGS84); 64.9599°N, 2.72820°E (ED50)
Water depth (m):	2145
Target drilling depth (mbsf):	400
Approved maximum penetration (mbsf):	400
Survey coverage (track map; seismic profile):	AMN17 (IL 6496 SP 940/IL 1214 SP 6496) Track map (Figure **AF5**) Seismic profiles (Figure **AF5**)
Objective(s):	To characterize age and lithology of initial basalt sequences on the Kolga High
Coring program:	Hole A: RCB to bit destruction or 400 mbsf
Downhole measurements program:	Triple combo, FMS-sonic-UBI, and VSP
Nature of rock anticipated:	Pliocene–Pleistocene mud (30 m) above Paleogene lava flows

Site VMVM-25A (Kolga High initial basalt)

Priority:	Alternate
Position:	64.9512°N, 2.72152°E (WGS84); 64.9515°N, 2.7235°E (ED50)
Water depth (m):	2160
Target drilling depth (mbsf):	400
Approved maximum penetration (mbsf):	400
Survey coverage (track map; seismic profile):	AMN17 (IL 6547 SP 940/XL 1214 SP 6547) Track map (Figure **AF6**) Seismic profiles (Figure **AF6**)
Objective(s):	To characterize age and lithology of initial basalt sequences on the Kolga High
Coring program:	Hole A: RCB to bit destruction or 400 mbsf
Downhole measurements program:	Triple combo, FMS-sonic-UBI, and VSP
Nature of rock anticipated:	Pliocene–Pleistocene mud (25 m) above Paleogene lava flows

Site VMVM-31A (North Modgunn Paleogene sediments)

Priority:	Primary
Position:	65.3642°N, 3.0543°E (WGS84); 65.3645°N, 3.0563°E (ED50)
Water depth (m):	1707
Target drilling depth (mbsf):	200
Approved maximum penetration (mbsf):	200
Survey coverage (track map; seismic profile):	AMN17 (IL 3966 SP 1291/XL 1565 SP 3966) Track map (Figure **AF7**) Seismic profiles (Figure **AF7**)
Objective(s):	To characterize age and lithology of Paleogene sediments in reference site
Coring program:	Hole A: APC/XCB to 200 mbsf; RCB to 200 mbsf if stiff sediments
Downhole measurements program:	Triple combo, FMS-sonic-UBI, and VSP
Nature of rock anticipated:	Pliocene–Pleistocene mud (55 m) above Paleogene mudstones

Site VMVM-32A (North Modgunn Paleogene sediments)

Priority:	Alternate
Position:	65.3714°N, 3.0585°E (WGS84); 65.3717°N, 3.0605°E (ED50)
Water depth (m):	1695
Target drilling depth (mbsf):	200
Approved maximum penetration (mbsf):	200
Survey coverage (track map; seismic profile):	AMN17 (IL 3922 SP 1291/XL 1565 SP 3922) Track map (Figure **AF8**) Seismic profiles (Figure **AF8**)
Objective(s):	To characterize age and lithology of Paleogene sediments in reference site
Coring program:	Hole A: APC/XCB to 200 mbsf; RCB to 200 mbsf if stiff sediments
Downhole measurements program:	Triple combo and FMS-sonic-UBI
Nature of rock anticipated:	Pliocene–Pleistocene mud (55 m) above Paleogene mudstones

Site VMVM-33A (North Modgunn Paleogene sediments)

Priority:	Alternate
Position:	65.4062°N, 3.09269°E (WGS84); 65.4065°N, 3.09470°E (ED50)
Water depth (m):	1673
Target drilling depth (mbsf):	200
Approved maximum penetration (mbsf):	200
Survey coverage (track map; seismic profile):	AMN17 (IL 3701 SP 1341/XL 1615 SP 3701) Track map (Figure **AF9**) Seismic profiles (Figure **AF9**)
Objective(s):	To characterize age and lithology of Paleogene sediments in reference site
Coring program:	Hole A: APC/XCB to 200 mbsf; RCB to 200 mbsf if stiff sediments
Downhole measurements program:	Triple combo and FMS-sonic-UBI
Nature of rock anticipated:	Pliocene–Pleistocene mud (110 m) above Paleogene mudstones

Site VMVM-40B (North Modgunn HTVC)

Priority:	Primary
Position:	65.3599°N, 3.0518°E (WGS84); 65.3602°N, 3.0538°E (ED50)
Water depth (m):	1696
Target drilling depth (mbsf):	200
Approved maximum penetration (mbsf):	200
Survey coverage (track map; seismic profile):	AMN17 (IL 3992 SP 1291/XL 1565 SP 3992) Track map (Figure **AF10**) Seismic profiles (Figure **AF10**)
Objective(s):	To characterize age and lithology of hydrothermal vent complex (HTVC) crater infill
Coring program:	Hole A: APC/XCB to 200 mbsf; RCB to 200 mbsf if stiff sediments
Downhole measurements program:	Triple combo, FMS-sonic-UBI, and VSP
Nature of rock anticipated:	Pliocene–Pleistocene mud (40 m) above Paleogene mudstones

Site VMVM-41A (North Modgunn HTVC)

Priority:	Alternate
Position:	65.3759°N, 3.0612°E (WGS84); 65.3762°N, 3.0632°E (ED50)
Water depth (m):	1686
Target drilling depth (mbsf):	200
Approved maximum penetration (mbsf):	200
Survey coverage (track map; seismic profile):	AMN17 (IL 3894 SP 1291/XL 1565 SP 3894) Track map (Figure **AF11**) Seismic profiles (Figure **AF11**)
Objective(s):	To characterize age and lithology of HTVC crater infill
Coring program:	Hole A: APC/XCB to 200 mbsf; RCB to 200 mbsf if stiff sediments
Downhole measurements program:	Triple combo, FMS-sonic-UBI, and VSP
Nature of rock anticipated:	Pliocene–Pleistocene mud (65 m) above Paleogene mudstones

Site VMVM-42A (North Modgunn HTVC)

Priority:	Alternate
Position:	65.4083°N, 3.07149°E (WGS84); 65.4086°N, 3.07350°E (ED50)
Water depth (m):	1695
Target drilling depth (mbsf):	300
Approved maximum penetration (mbsf):	300
Survey coverage (track map; seismic profile):	AMN17 (IL 3701 SP 1260/XL 1534 SP 3701) Track map (Figure **AF12**) Seismic profiles (Figure **AF12**)
Objective(s):	To characterize age and lithology of HTVC crater infill
Coring program:	Hole A: APC/XCB to 300 mbsf; RCB to 300 mbsf if stiff sediments
Downhole measurements program:	Triple combo, FMS-sonic-UBI, and VSP
Nature of rock anticipated:	Pliocene–Pleistocene mud (135 m) above Paleogene mudstones

Site VMVM-51A (Mimir High)

Priority:	Alternate
Position:	65.8732°N, 1.95852°E (WGS84); 65.8735°N, 1.9606°E (ED50)
Water depth (m):	2147
Target drilling depth (mbsf):	800
Approved maximum penetration (mbsf):	800
Survey coverage (track map; seismic profile):	MNR11-7324 7178/JC IL 14213 SP 24851 Track map (Figure **AF13**) Seismic profiles (Figure **AF13**)
Objective(s):	To characterize Paleogene sediments and PETM interval
Coring program:	Hole A: APC/XCB to 800 mbsf Hole B: RCB to 800 mbsf
Downhole measurements program:	Triple combo, FMS-sonic-UBI, and VSP
Nature of rock anticipated:	Pliocene–Pleistocene mud (200 m) above Paleogene mudstones

Site VMVM-55B (Mimir High)

Priority:	Primary
Position:	65.8313°N, 2.02682°E (WGS84); 65.8316°N, 2.02890°E (ED50)
Water depth (m):	2186
Target drilling depth (mbsf):	800
Approved maximum penetration (mbsf):	800
Survey coverage (track map; seismic profile):	MNR07-7319 15560 Track map (Figure **AF14**) Seismic profiles (Figure **AF14**)
Objective(s):	To characterize Paleogene sediments and PETM interval
Coring program:	Hole A: APC/XCB to 800 mbsf Hole B: RCB to 800 mbsf
Downhole measurements program:	Triple combo, FMS-sonic-UBI, and VSP
Nature of rock anticipated:	Pliocene–Pleistocene mud (255 m) above Paleogene mudstones

Site VMVM-56A ribbon start (Mimir High)

Priority:	Alternate
Position:	65.8280°N, 1.9560°E (WGS84); 65.8283°N, 1.95810°E (ED50)
Water depth (m):	2285
Target drilling depth (mbsf):	200
Approved maximum penetration (mbsf):	200
Survey coverage (track map; seismic profile):	MNR07-7319 15300 Track map (Figure **AF15**) Seismic profiles (Figure **AF15**)
Objective(s):	To characterize Paleogene sediments and PETM interval
Coring program:	Hole A: APC/XCB to 200 mbsf; RCB to 200 mbsf if stiff sediments
Downhole measurements program:	Triple combo and FMS-sonic-UBI
Nature of rock anticipated:	Pliocene–Pleistocene mud above Paleogene mudstones

Site VMVM-56A ribbon end (Mimir High)

Priority:	Alternate
Position:	65.8301°N, 1.99962°E (WGS84); 65.8304°N, 2.0017°E (ED50)
Water depth (m):	2203
Target drilling depth (mbsf):	200
Approved maximum penetration (mbsf):	200
Survey coverage (track map; seismic profile):	MNR07-7319 15460 Track map (Figure **AF16**) Seismic profiles (Figure **AF16**)
Objective(s):	To characterize Paleogene sediments and PETM interval
Coring program:	Hole A: APC/XCB to 200 mbsf; RCB to 200 mbsf if stiff sediments
Downhole measurements program:	Triple combo and FMS-sonic-UBI
Nature of rock anticipated:	Pliocene–Pleistocene mud above Paleogene mudstones

Site VMVM-61A (Skoll High basalt Sequence 1)

Priority:	Primary
Position:	67.3067°N, 3.73746°E (WGS84); 67.3069°N, 3.7396°E (ED50)
Water depth (m):	1200
Target drilling depth (mbsf):	300
Approved maximum penetration (mbsf):	300
Survey coverage (track map; seismic profile):	CVX1101 (IL 1852 SP 3267/XL 5057 SP 1062) Track map (Figure **AF17**) Seismic profiles (Figure **AF17**)
Objective(s):	To sample basaltic lava flows, Sequence 1
Coring program:	Hole A: RCB to 300 mbsf
Downhole measurements program:	Triple combo, FMS-sonic-UBI, and VSP
Nature of rock anticipated:	Postbreakup sediments (125 m) above basaltic basement

Site VMVM-62A (Skoll High basalt Sequence 1)

Priority:	Alternate
Position:	67.2891°N, 3.67576°E (WGS84); 67.2893°N, 3.6779°E (ED50)
Water depth (m):	1198
Target drilling depth (mbsf):	300
Approved maximum penetration (mbsf):	300
Survey coverage (track map; seismic profile):	CVX1101 (IL 1832 SP 3006/XL 4796 SP 1042) Track map (Figure **AF18**) Seismic profiles (Figure **AF18**)
Objective(s):	To sample basaltic lava flows, Sequence 1
Coring program:	Hole A: RCB to 300 mbsf
Downhole measurements program:	Triple combo, FMS-sonic-UBI, and VSP
Nature of rock anticipated:	Postbreakup sediments (115 m) above basaltic basement

Site VMVM-07A (Skoll High basalt Sequence 2)

Priority:	Primary
Position:	67.3308°N, 3.61935°E (WGS84); 67.3310°N, 3.62150°E (ED50)
Water depth (m):	1206
Target drilling depth (mbsf):	400
Approved maximum penetration (mbsf):	400
Survey coverage (track map; seismic profile):	CVX1101 (IL 2041 SP 2436/XL 4796 SP 1251) Track map (Figure **AF19**) Seismic profiles (Figure **AF19**)
Objective(s):	To sample basaltic lava flows, Sequence 2
Coring program:	Hole A: RCB to 400 mbsf
Downhole measurements program:	Triple combo, FMS-sonic-UBI, and VSP
Nature of rock anticipated:	Postbreakup sediments (220 m) above basaltic basement

Site VMVM-71A (Skoll High basalt Sequence 2)

Priority:	Alternate
Position:	67.3384°N, 3.69456°E (WGS84); 67.3386°N, 3.6967°E (ED50)
Water depth (m):	1200
Target drilling depth (mbsf):	400
Approved maximum penetration (mbsf):	400
Survey coverage (track map; seismic profile):	CVX1101 (IL 2012 SP 3267/XL 5057 SP 1222) Track map (Figure **AF20**) Seismic profiles (Figure **AF20**)
Objective(s):	To sample basaltic lava flows, Sequence 2
Coring program:	Hole A: RCB to 400 mbsf
Downhole measurements program:	Triple combo, FMS-sonic-UBI, and VSP
Nature of rock anticipated:	Postbreakup sediments (195 m) above basaltic basement

Site VMVM-80A (Outer High)

Priority:	Primary
Position:	68.6002°N, 4.64057°E (WGS84); 68.6004°N, 4.6428°E (ED50)
Water depth (m):	2864
Target drilling depth (mbsf):	310
Approved maximum penetration (mbsf):	310
Survey coverage (track map; seismic profile):	HV96-7 SP 4728 Track map (Figure **AF21**) Seismic profiles (Figure **AF21**)
Objective(s):	To sample Outer High volcanogenic rocks
Coring program:	Hole A: RCB to 310 mbsf
Downhole measurements program:	Triple combo and FMS-sonic-UBI
Nature of rock anticipated:	Postbreakup sediments (210 m) above basaltic basement

Site VMVM-81A (Outer High)

Priority:	Alternate
Position:	68.6264°N, 4.58257°E (WGS84); 68.6266°N, 4.5848°E (ED50)
Water depth (m):	2913
Target drilling depth (mbsf):	200
Approved maximum penetration (mbsf):	200
Survey coverage (track map; seismic profile):	HV96-7 SP 5030 Track map (Figure **AF22**) Seismic profiles (Figure **AF22**)
Objective(s):	To sample Outer High volcanogenic rocks
Coring program:	Hole A: RCB to 200 mbsf
Downhole measurements program:	Triple combo and FMS-sonic-UBI
Nature of rock anticipated:	Postbreakup sediments (55 m) above basaltic basement

Site VMVM-09A (Outer SDR)

Priority:	Primary
Position:	68.7604°N, 5.79491°E (WGS84); 68.7605°N, 5.79710°E (ED50)
Water depth (m):	3156
Target drilling depth (mbsf):	550
Approved maximum penetration (mbsf):	550
Survey coverage (track map; seismic profile):	HV96-6 SP 2355 Track map (Figure **AF23**) Seismic profiles (Figure **AF23**)
Objective(s):	To sample Outer SDR basalts
Coring program:	Hole A: RCB to 550 mbsf
Downhole measurements program:	Triple combo, FMS-sonic-UBI, and VSP
Nature of rock anticipated:	Postbreakup sediments (450 m) above basaltic basement

Site VMVM-10B (Outer SDR)

Priority:	Alternate
Position:	68.8304°N, 4.12833°E (WGS84); 68.8306°N, 4.13060°E (ED50)
Water depth (m):	3237
Target drilling depth (mbsf):	750
Approved maximum penetration (mbsf):	750
Survey coverage (track map; seismic profile):	HV96-7 SP 7370/HV96-8 SP 495 Track map (Figure **AF24**) Seismic profiles (Figure **AF24**)
Objective(s):	To sample Outer SDR basalts
Coring program:	Hole A: RCB to 750 mbsf
Downhole measurements program:	Triple combo, FMS-sonic-UBI, and VSP
Nature of rock anticipated:	Postbreakup sediments (650 m) above basaltic basement

Hole 642E

Priority:	Alternate
Position (642E):	67°13.200′N, 2°55.800′E (WGS84)
Water depth (m):	1272
Target drilling depth (mbsf):	Not applicable (NA)
Approved maximum penetration (mbsf):	NA
Survey coverage (track map; seismic profile):	NA
Objective(s):	Log in Hole 642E
Coring program:	None
Downhole measurements program:	Triple combo, FMS-sonic-UBI, and VSP
Nature of rock anticipated:	Reentry of Hole 642E for temperature and logging

Figure AF1. Track map and seismic profiles, primary Proposed Site VMVM-20A. SP = shotpoint. SSDB = Site Survey Data Bank.

Site Figure for VMVM-20A | Primary

Coordinates: 64.96270° N, 002.74982° E (WGS84)
Water depth: 2077 m
Penetration: 200 m

Data

Remarks: Three 3D seismic volumes are available in the area: shallow high resolution (HiRes), processed migration stack (PRCMIG) and full-fast-track (FFT).

Site location:
AMN17-PRCMIG-Inline_6464 (SP-1020) // AMN17-PRCMIG-Xline_1294 (SP-6464)

Data files in SSDB: Seismic SEG-Y profiles extracted from 3D cube, velocity data.

Additional data: Velocity cube, gravity and magnetic grids.

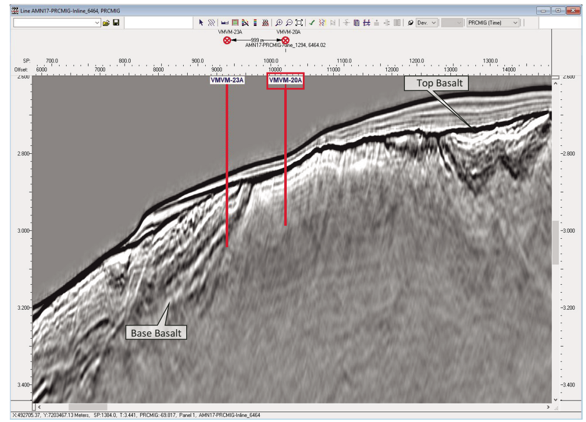

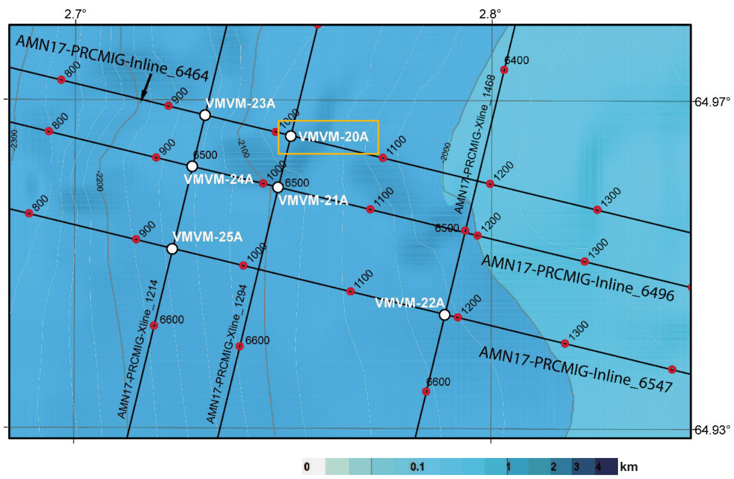

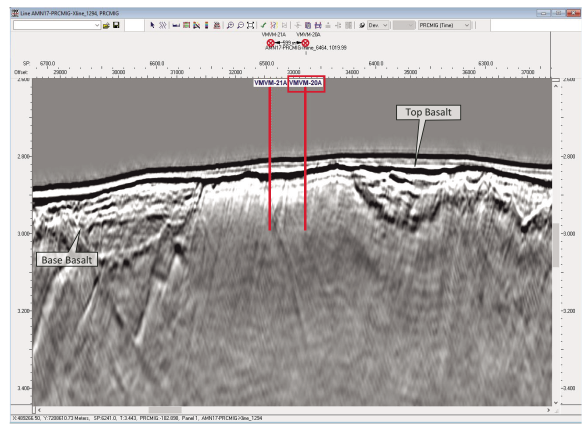

Figure AF2. Track map and seismic profiles, alternate Proposed Site VMVM-21A. SP = shotpoint. SSDB = Site Survey Data Bank.

Site Figure for VMVM-21A | Alternate

Coordinates: 64.95750° N, 002.74682° E (WGS84)
Water depth: 2078 m
Penetration: 200 m

Data

Remarks: Three 3D seismic volumes are available in the area: shallow high resolution (HiRes), processed migration stack (PRCMIG) and full-fast-track (FFT)

Site location:
AMN17-PRCMIG-Inline_6496 (SP-1020) // AMN17-PRCMIG-Xline_1294 (SP-6469)

Data files in SSDB: Seismic SEG-Y profiles extracted from 3D cube, velocity data.

Additional data: Velocity cube, gravity and magnetic grids.

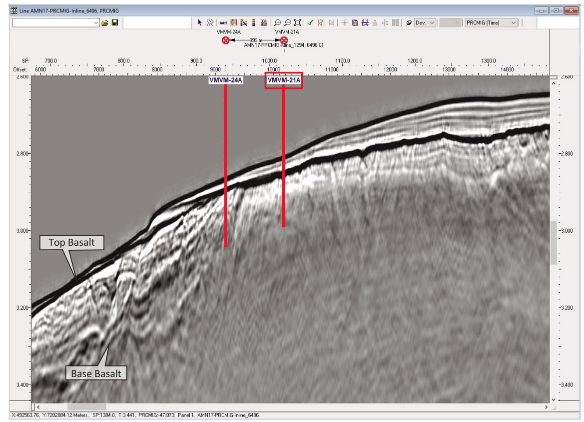

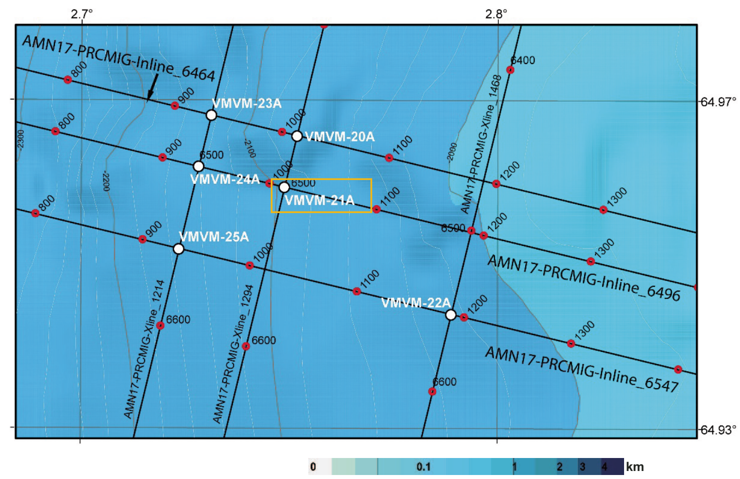

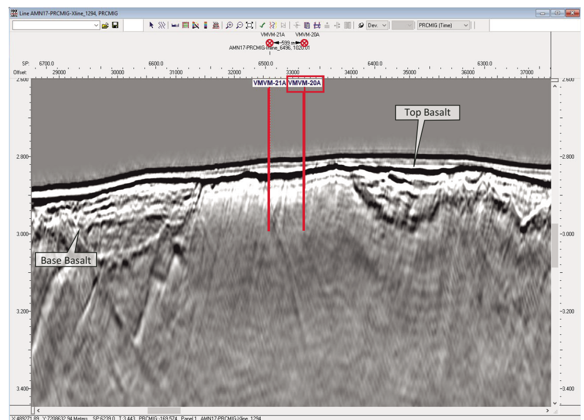

Figure AF3. Track map and seismic profiles, alternate Proposed Site VMVM-22A. SP = shotpoint. SSDB = Site Survey Data Bank.

Site Figure for VMVM-22A | Alternate

Coordinates: 64.94460° N, 002.78692 (WGS84)
Water depth: 2017 m
Penetration: 200 m

Data

Remarks: Three 3D seismic volumes are available in the area: shallow high resolution (HiRes), processed migration stack (PRCMIG) and full-fast-track (FFT).

Site location:
AMN17-PRCMIG-Inline_6547 (SP-1194) // AMN17-PRCMIG-Xline_1468 (SP-6547)

Data files in SSDB: Seismic SEG-Y profiles extracted from 3D cube, velocity data.

Additional data: Velocity cube, gravity and magnetic grids.

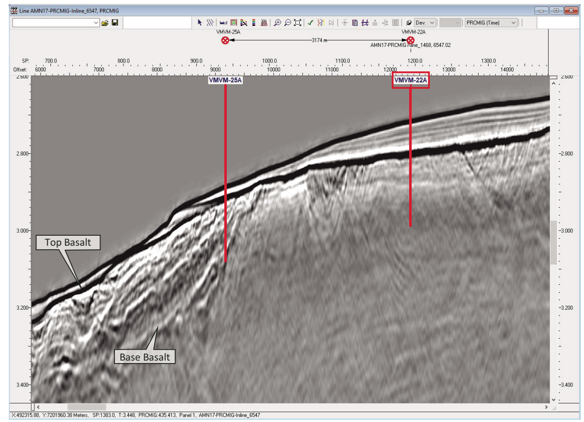

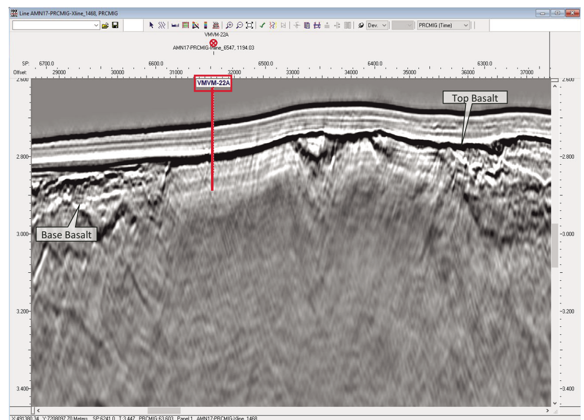

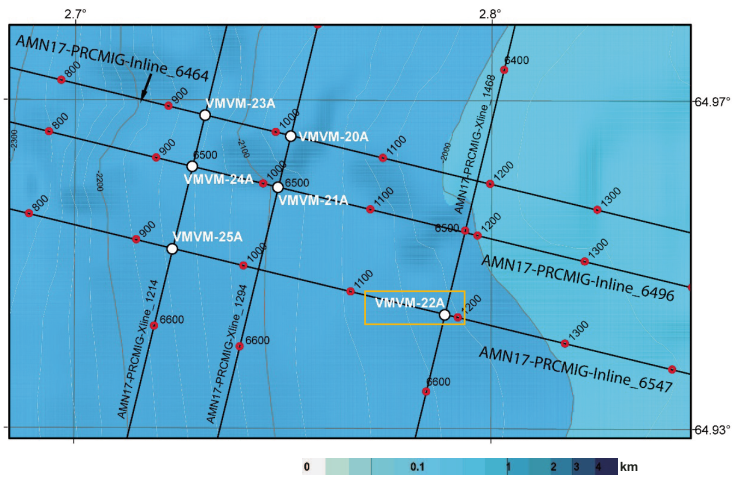

Figure AF4. Track map and seismic profiles, primary Proposed Site VMVM-23A. SP = shotpoint. SSDB = Site Survey Data Bank.

Site Figure for VMVM-23A | Primary

Coordinates: 64.96480° N, 002.72922° E (WGS84)
Water depth: 2137 m
Penetration: 400 m

Data

Remarks: Three 3D seismic volumes are available in the area: shallow high resolution (HiRes), processed migration stack (PRCMIG) and full-fast-track (FFT).

Site location:
AMN17-PRCMIG-Inline_6464 (SP-940) // AMN17-PRCMIG-Xline_1214 (SP-6464)

Data files in SSDB: Seismic SEG-Y profiles extracted from 3D cube, velocity data.

Additional data: Velocity cube, gravity and magnetic grids.

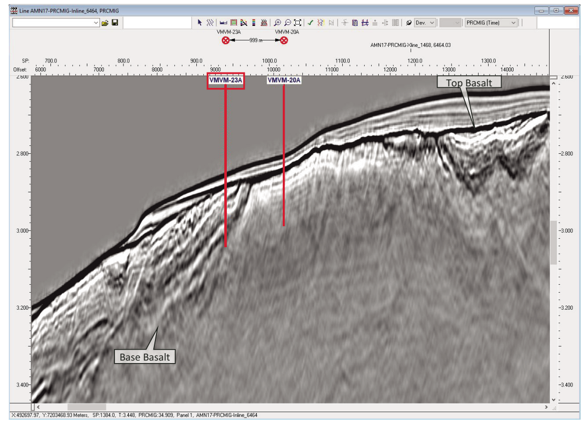

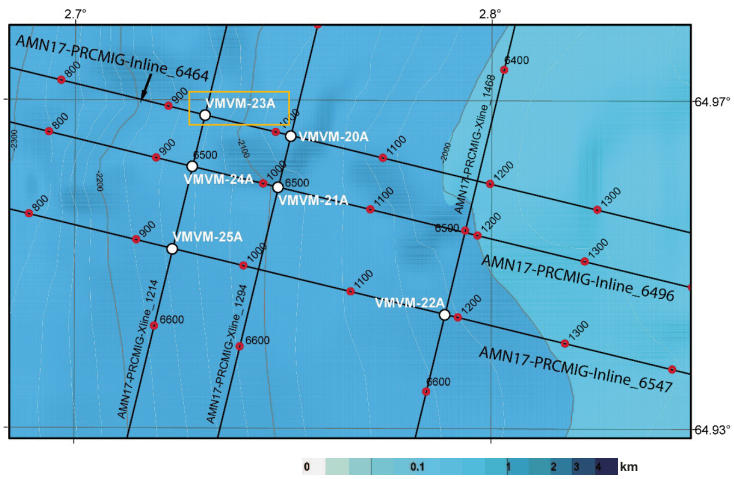

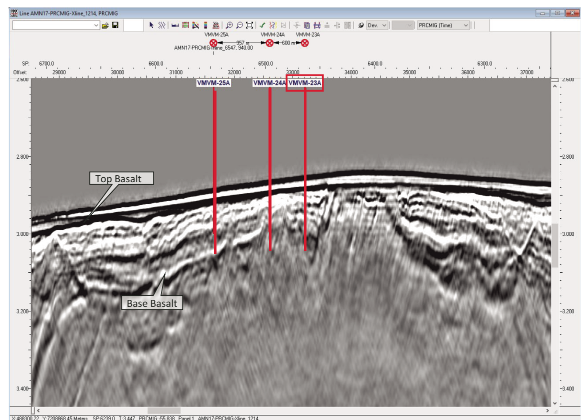

Figure AF5. Track map and seismic profiles, alternate Proposed Site VMVM-24A. SP = shotpoint. SSDB = Site Survey Data Bank.

Site Figure for VMVM-24A | Alternate

Coordinates: 64.95960° N, 002.72622° E (WGS84)
Water depth: 2145 m
Penetration: 400 m

Data

Remarks: Three 3D seismic volumes are available in the area: shallow high resolution (HiRes), processed migration stack (PRCMIG) and full-fast-track (FFT).

Site location:
AMN17-PRCMIG-Inline_6496 (SP-940) // AMN17-PRCMIG-Xline_1214 (SP-6469)

Data files in SSDB: Seismic SEG-Y profiles extracted from 3D cube, velocity data.

Additional data: Velocity cube, gravity and magnetic grids.

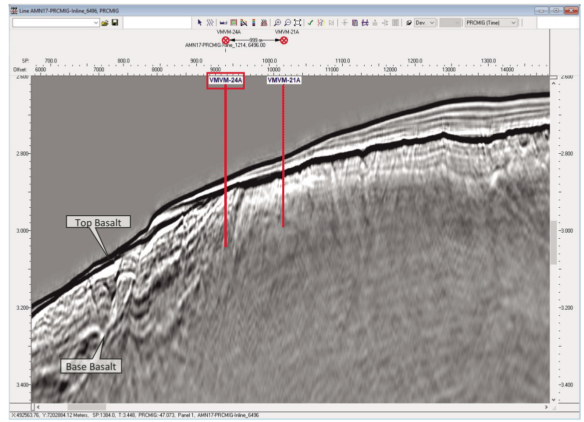

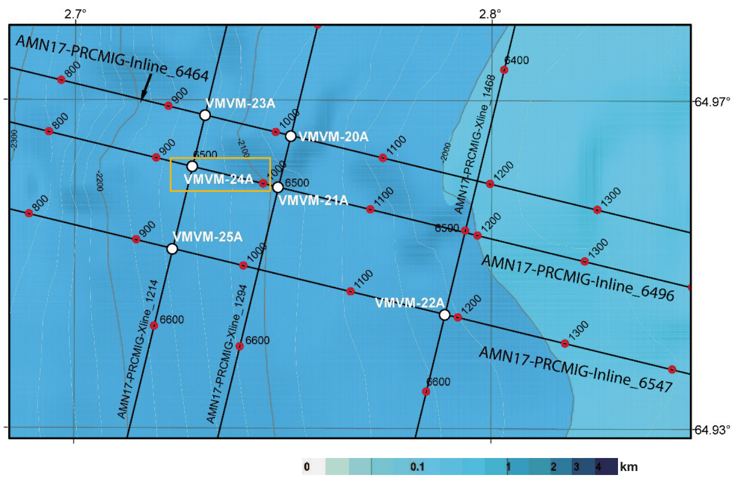

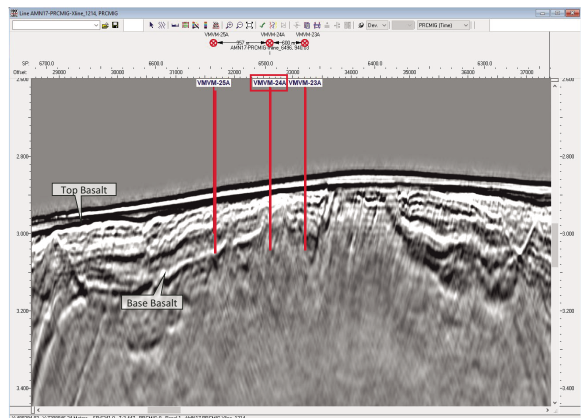

Figure AF6. Track map and seismic profiles, alternate Proposed Site VMVM-25A. SP = shotpoint. SSDB = Site Survey Data Bank.

Site Figure for VMVM-25A | Alternate

Coordinates: 64.95120° N, 2.72152° E (WGS84)
Water depth: 2160 m
Penetration: 400 m

Data

Remarks: Three 3D seismic volumes are available in the area: shallow high resolution (HiRes), processed migration stack (PRCMIG) and full-fast-track (FFT).

Site location:
AMN17-PRCMIG-Inline_6547 (SP-940) // AMN17-PRCMIG-Xline_1214 (SP-6547)

Data files in SSDB: Seismic SEG-Y profiles extracted from 3D cube, velocity data.

Additional data: Velocity cube, gravity and magnetic grids.

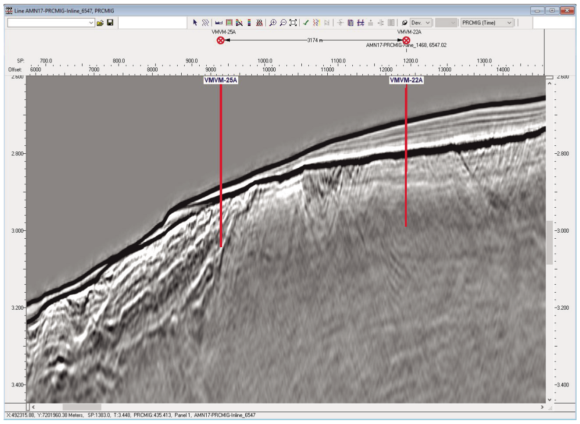

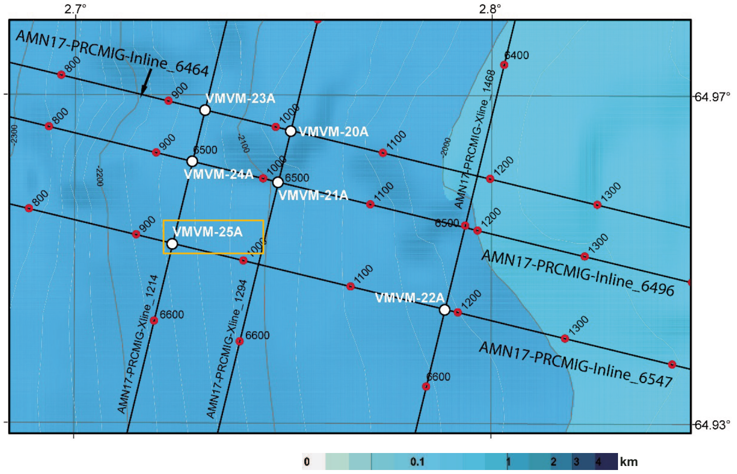

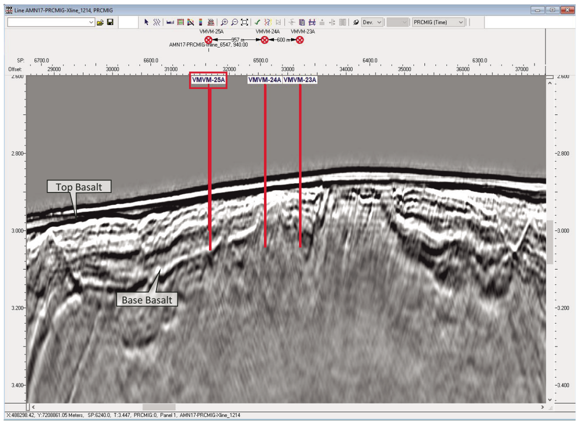

Figure AF7. Track map and seismic profiles, primary Proposed Site VMVM-31A. SP = shotpoint. SSDB = Site Survey Data Bank.

Site Figure for VMVM-31A | Primary

Coordinates: 65.36420° N, 3.05430° E (WGS84)
Water depth: 1707 m
Penetration: 200 m

Data

Remarks: Three 3D seismic volumes are available in the area: shallow high resolution (HiRes), processed migration stack (PRCMIG) and full-fast-track (FFT).

Site location:
AMN17-PRCMIG-Inline_3966 (SP-1291) // AMN17-PRCMIG-Xline_1565 (SP-3966)

Data files in SSDB: Seismic SEG-Y profiles extracted from 3D cube, velocity data.

Additional data: Velocity cube, gravity and magnetic grids.

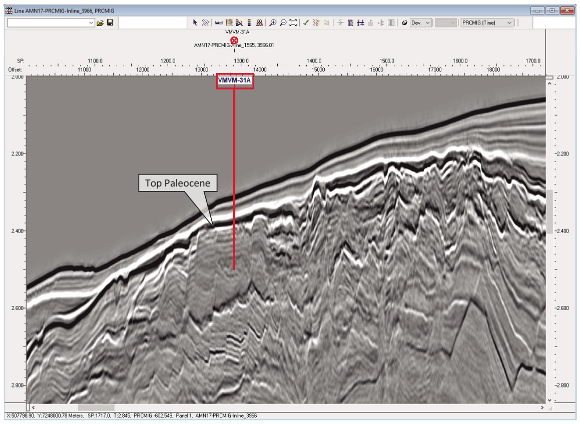

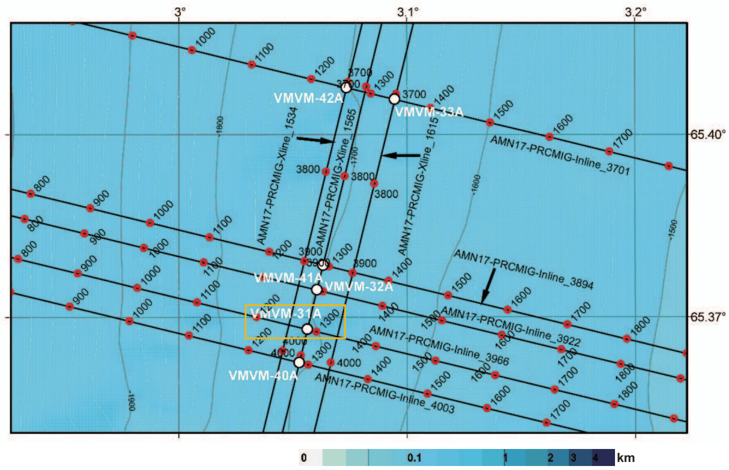

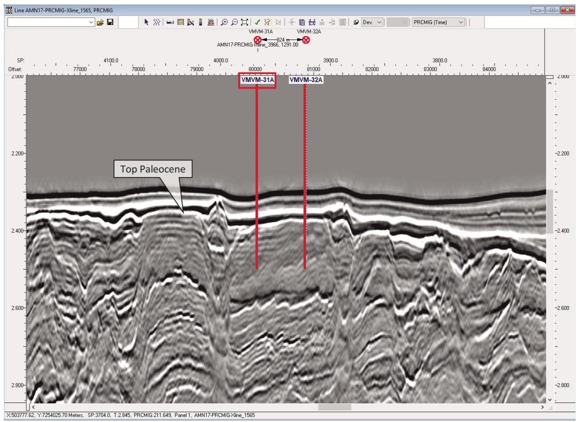

Figure AF8. Track map and seismic profiles, alternate Proposed Site VMVM-32A. SP = shotpoint. SSDB = Site Survey Data Bank.

Site Figure for VMVM-32A | Alternate

Coordinates: 65.37140° N, 3.05850° E (WGS84)
Water depth: 1695 m
Penetration: 200 m

Data

Remarks: Three 3D seismic volumes are available in the area: shallow high resolution (HiRes), processed migration stack (PRCMIG) and full-fast-track (FFT).

Site location:
AMN17-PRCMIG-Inline_3922 (SP-1291) // AMN17-PRCMIG-Xline_1565 (SP-3922)

Data files in SSDB: Seismic SEG-Y profiles extracted from 3D cube, velocity data.

Additional data: Velocity cube, gravity and magnetic grids.

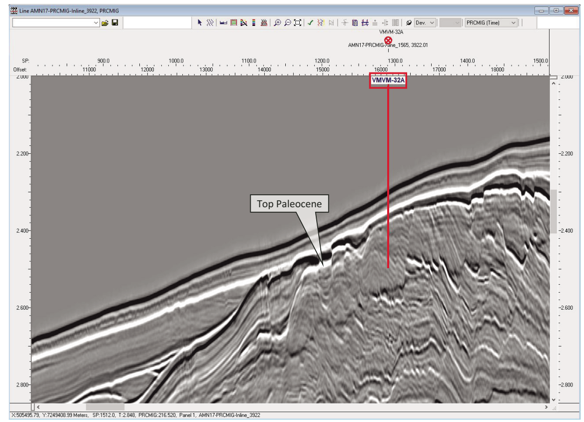

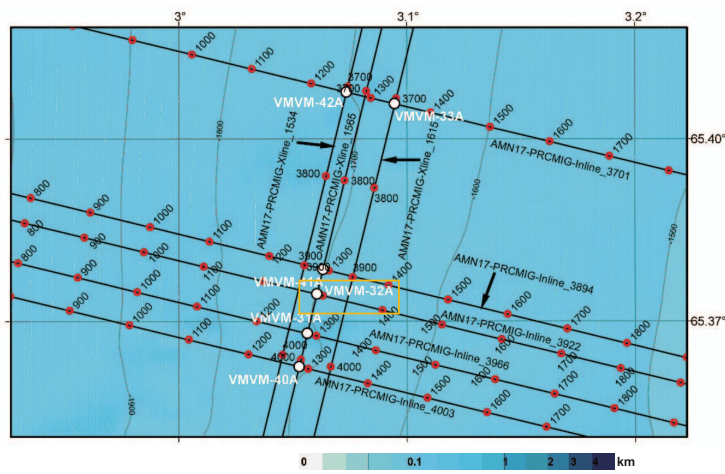

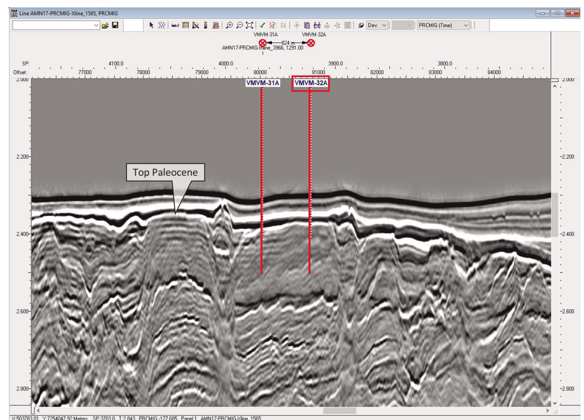

Figure AF9. Track map and seismic profiles, alternate Proposed Site VMVM-33A. SP = shotpoint. SSDB = Site Survey Data Bank.

Site Figure for VMVM-33A | Alternate

Coordinates: 65.40620° N, 3.09269° E (WGS84)
Water depth: 1673 m
Penetration: 200 m

Data

Remarks: Three 3D seismic volumes are available in the area: shallow high resolution (HiRes), processed migration stack (PRCMIG) and full-fast-track (FFT).

Site location:
AMN17-PRCMIG-Inline_3701 (SP-1341) // AMN17-PRCMIG-Xline_1615 (SP-3701)

Data files in SSDB: Seismic SEG-Y profiles extracted from 3D cube, velocity data.

Additional data: Velocity cube, gravity and magnetic grids.

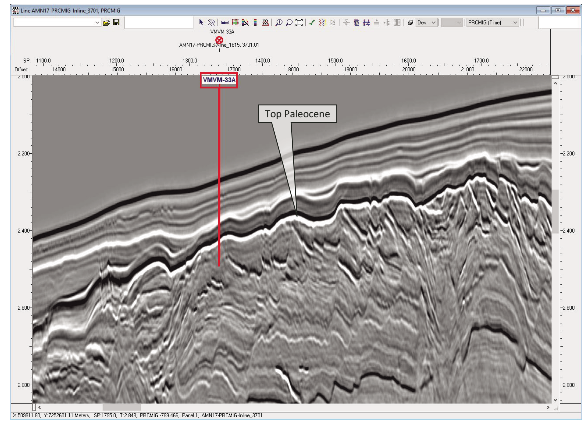

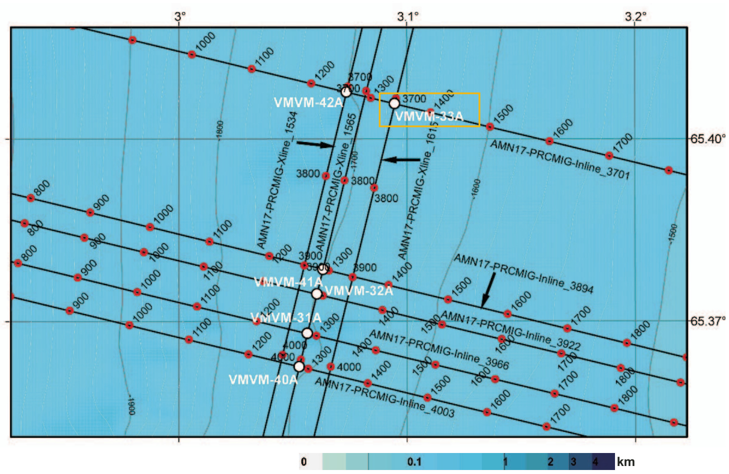

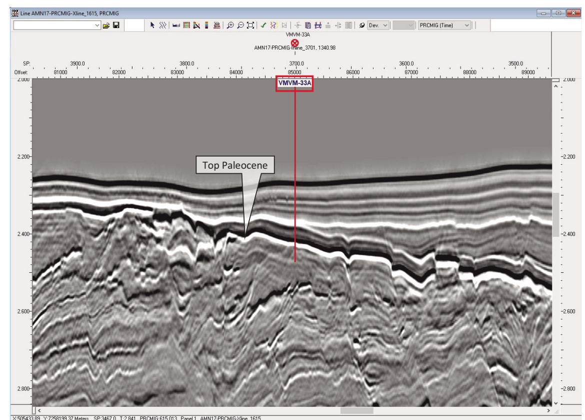

Figure AF10. Track map and seismic profiles, primary Proposed Site VMVM-40B. SP = shotpoint. SSDB = Site Survey Data Bank.

Site Figure for VMVM-40B | Primary

Coordinates: 65.35990° N, 3.05180° E (WGS84)
Water depth: 1696 m
Penetration: 200 m

Data

Remarks: Three 3D seismic volumes are available in the area: shallow high resolution (HiRes), processed migration stack (PRCMIG) and full-fast-track (FFT).

Site location:
AMN17-PRCMIG-Inline_3992 (SP-1291) // AMN17-PRCMIG-Xline_1565 (SP-3992)

Data files in SSDB: Seismic SEG-Y profiles extracted from 3D cube, velocity data.

Additional data: Velocity cube, gravity and magnetic grids.

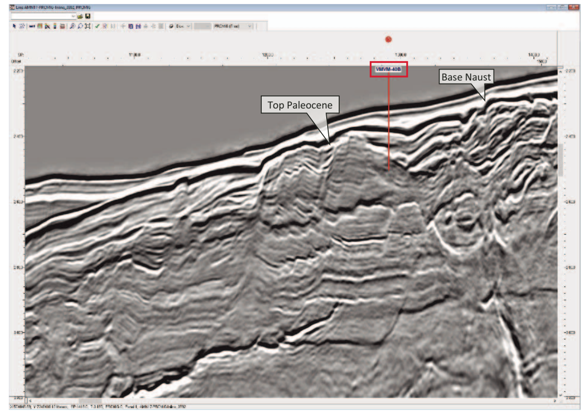

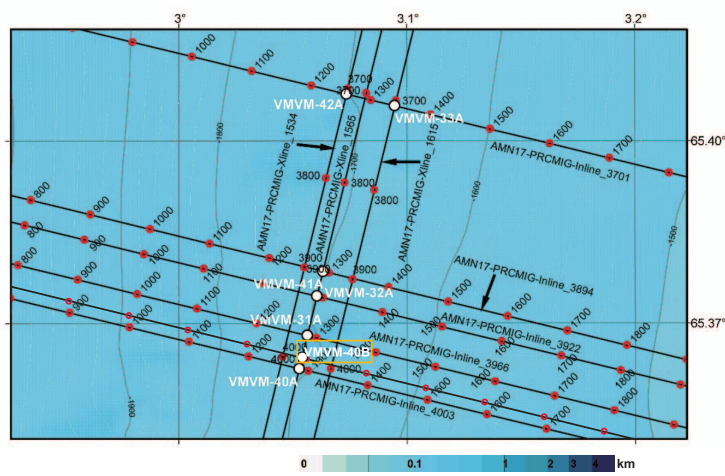

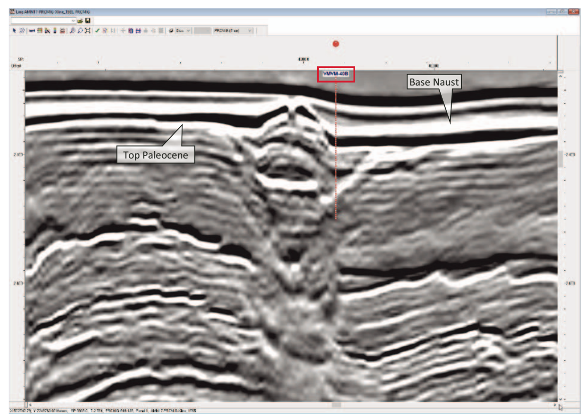

Figure AF11. Track map and seismic profiles, alternate Proposed Site VMVM-41A. SP = shotpoint. SSDB = Site Survey Data Bank.

Site Figure for VMVM-41A | Alternate

Coordinates: 65.37590° N, 3.06120° E (WGS84)
Water depth: 1686 m
Penetration: 200 m

Data

Remarks: Three 3D seismic volumes are available in the area: shallow high resolution (HiRes), processed migration stack (PRCMIG) and full-fast-track (FFT).

Site location:
AMN17-PRCMIG-Inline_3894 (SP-1291) // AMN17-PRCMIG-Xline_1565 (SP-3894)

Data files in SSDB: Seismic SEG-Y profiles extracted from 3D cube, velocity data.

Additional data: Velocity cube, gravity and magnetic grids.

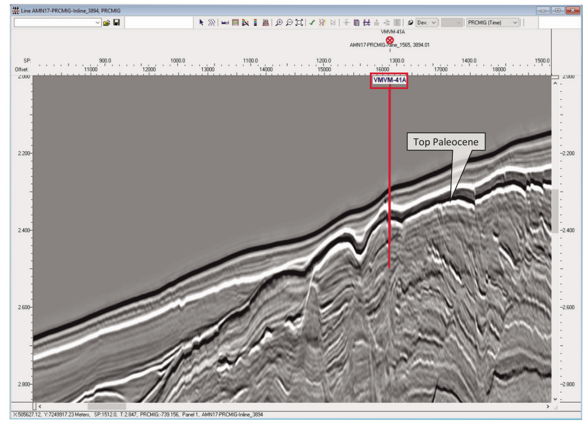

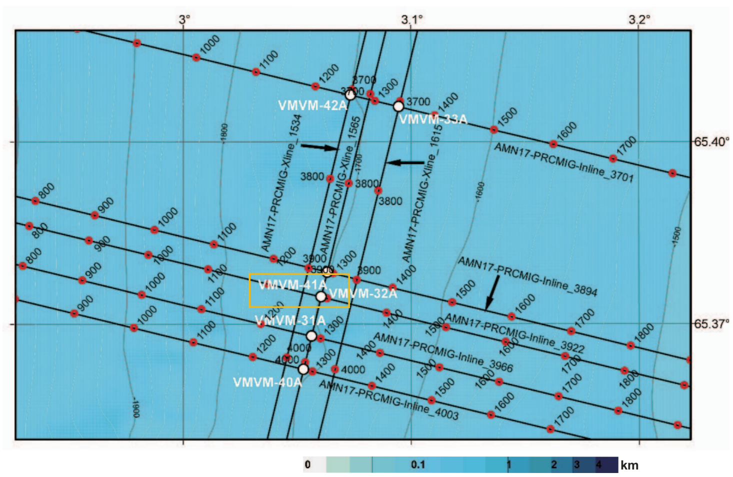

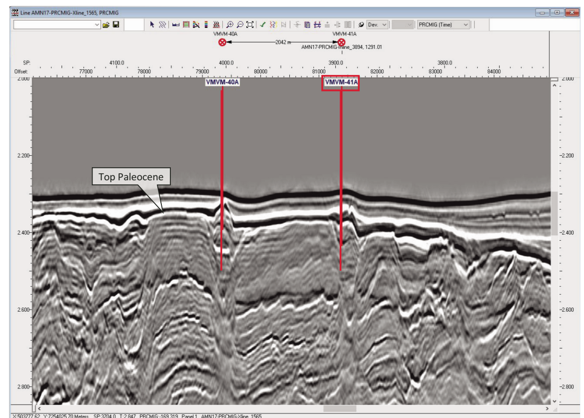

Figure AF12. Track map and seismic profiles, alternate Proposed Site VMVM-42A. SP = shotpoint. SSDB = Site Survey Data Bank.

Site Figure for VMVM-42A | Alternate

Coordinates: 65.40830° N, 3.07149° E (WGS84)
Water depth: 1695 m
Penetration: 300 m

Data

Remarks: Three 3D seismic volumes are available in the area: shallow high resolution (HiRes), processed migration stack (PRCMIG) and full-fast-track (FFT).

Site location:
AMN17-PRCMIG-Inline_3701 (SP-1260) // AMN17-PRCMIG-Xline_1534 (SP-3701)

Data files in SSDB: Seismic SEG-Y profiles extracted from 3D cube, velocity data.

Additional data: Velocity cube, gravity and magnetic grids.

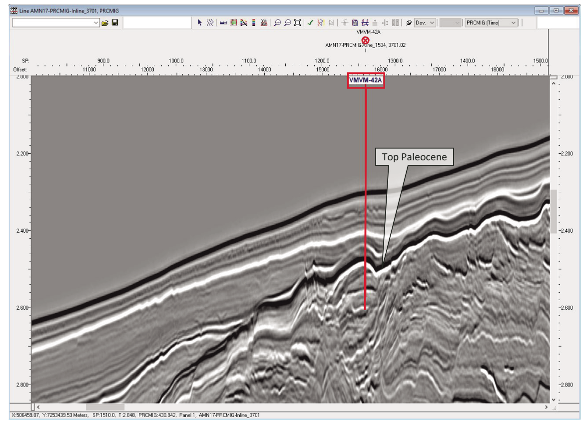

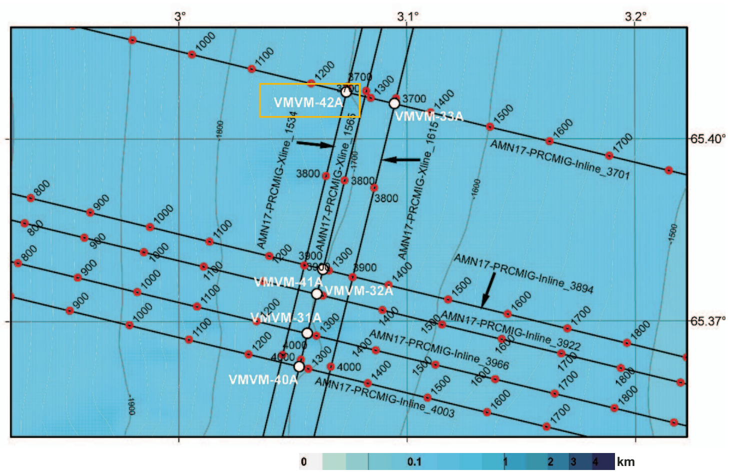

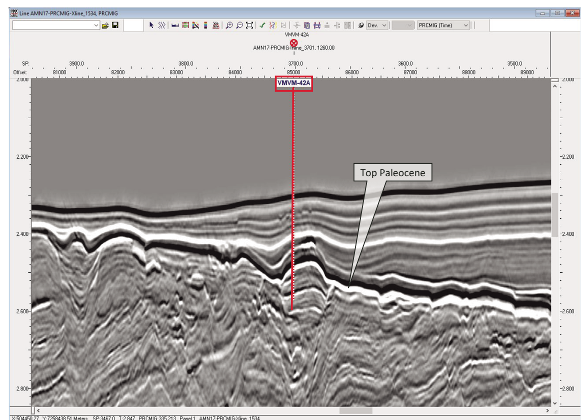

Figure AF13. Track map and seismic profiles, alternate Proposed Site VMVM-51A. SP = shotpoint. SSDB = Site Survey Data Bank.

Site Figure for VMVM-51A | Alternate

Coordinates: 65.87320° N, 1.95852° E (WGS84)
Water depth: 2147 m
Penetration: 800 m

Data

Remarks: 2D seismic survey and J-Cube MN volume are available in the area: Clari-Fi broadband reprocessed and processed migration stack (PRCMIG) respectively.

Site location:
CFI-MNR11-7324 (SP-7178) // J-Cube MN-PRCMIG-Xline_14213 (SP-24851)

Data files in SSDB: Seismic 2D SEG-Y profile and crossline extracted from J-Cube MN.

Additional data: Velocity cube, gravity grids, magnetic grids and seafloor sampling report (VTMS00).

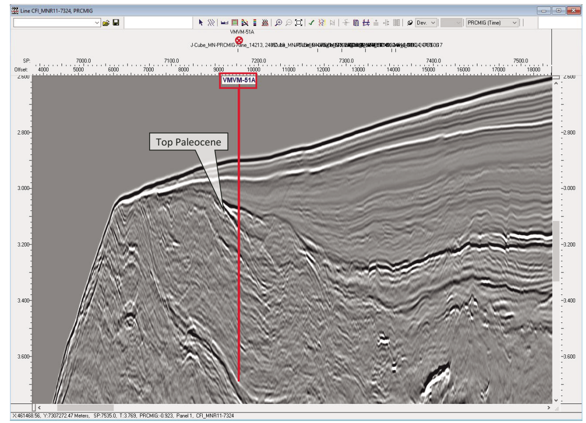

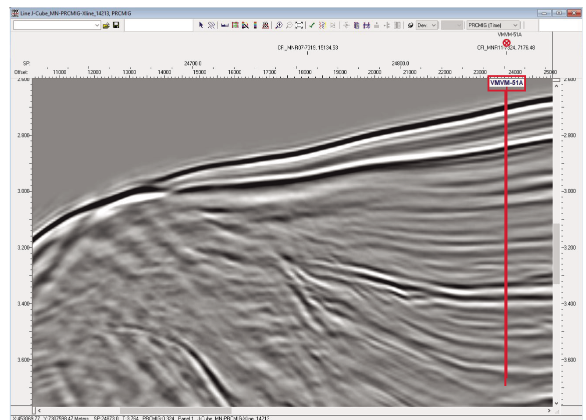

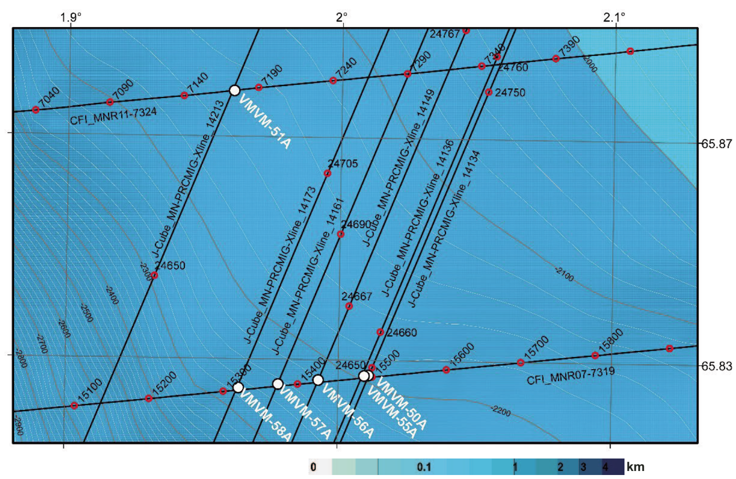

Figure AF14. Track map and seismic profile, primary Proposed Site VMVM-55B. SP = shotpoint. SSDB = Site Survey Data Bank.

Site Figure for VMVM-55B | Primary

Coordinates: 65.83130° N, 2.02682° E (WGS84)
Water depth: 2186 m
Penetration: 800 m

Data

Remarks: 2D seismic survey and J-Cube MN volume are available in the area: Clari-Fi broadband reprocessed and processed migration stack (PRCMIG) respectively.

Site location:
CFI-MNR07-7319 (SP-15560)

Data files in SSDB: Seismic 2D SEG-Y profile.

Additional data: Velocity cube, gravity grids, magnetic grids and seafloor sampling report (VTMS00).

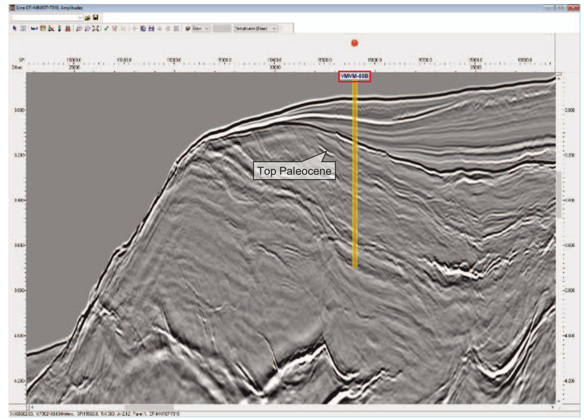

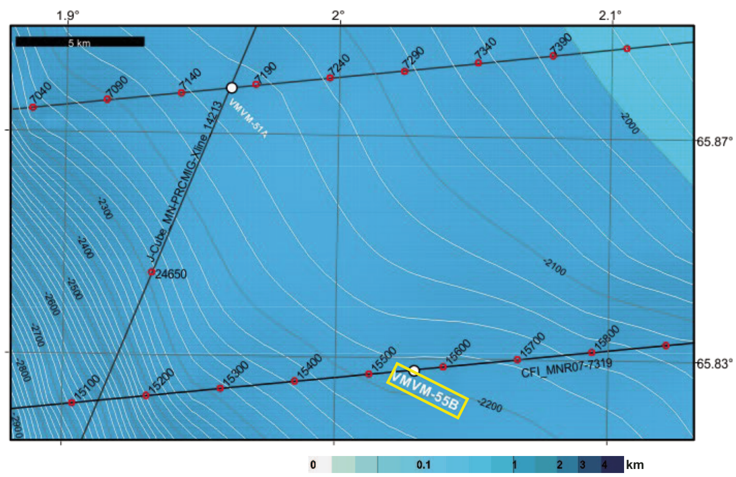

Figure AF15. Track map and seismic profile, alternate Proposed Site VMVM-56A ribbon start. SP = shotpoint. SSDB = Site Survey Data Bank.

Site Figure for VMVM-56A; Start | Ribbon

Coordinates: 65.82800° N, 1.95602° E (WGS84)
Water depth: 2285 m
Penetration: 200 m

Data

Remarks: 2D seismic survey and J-Cube MN volume are available in the area: Clari-Fi broadband reprocessed and processed migration stack (PRCMIG) respectively.

Site location:
CFI-MNR07-7319 (SP-15300)

Data files in SSDB: Seismic 2D SEG-Y profile.

Additional data: Velocity cube, gravity grids, magnetic grids and seafloor sampling report (VTMS00).

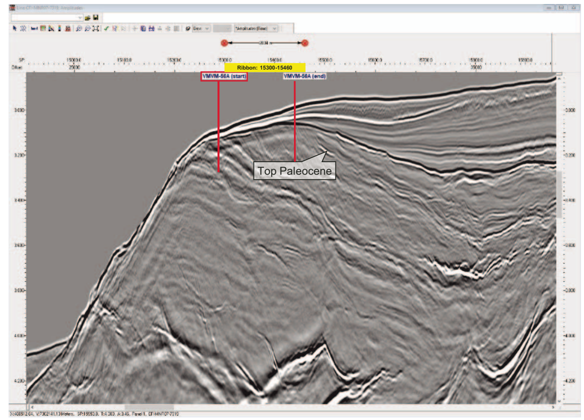

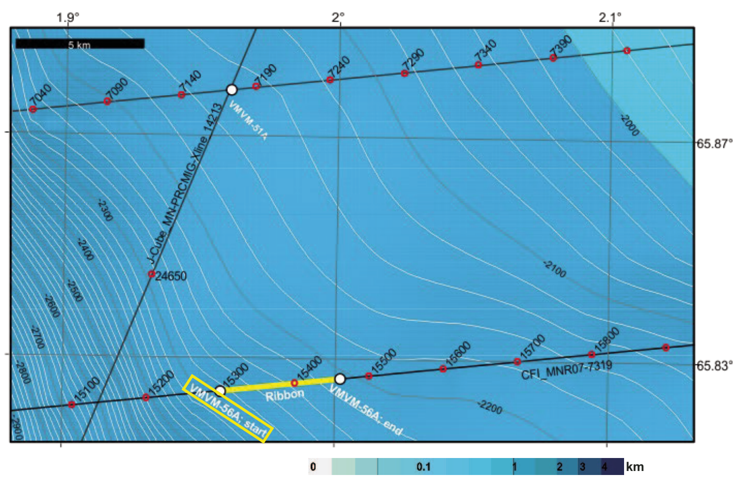

Figure AF16. Track map and seismic profile, alternate Proposed Site VMVM-56A ribbon end. SP = shotpoint. SSDB = Site Survey Data Bank.

Site Figure for VMVM-56A; End | Ribbon

Coordinates: 65.83010° N, 1.99962° E (WGS84)
Water depth: 2203 m
Penetration: 200 m

Data

Remarks: 2D seismic survey and J-Cube MN volume are available in the area: Clari-Fi broadband reprocessed and processed migration stack (PRCMIG) respectively.

Site location:
CFI-MNR07-7319 (SP-15460)

Data files in SSDB: Seismic 2D SEG-Y profile.

Additional data: Velocity cube, gravity grids, magnetic grids and seafloor sampling report (VTMS00).

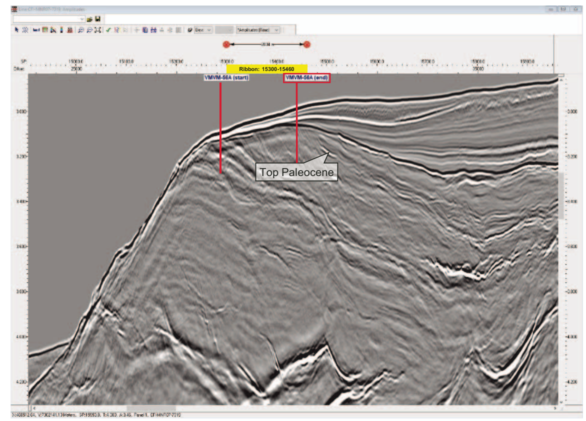

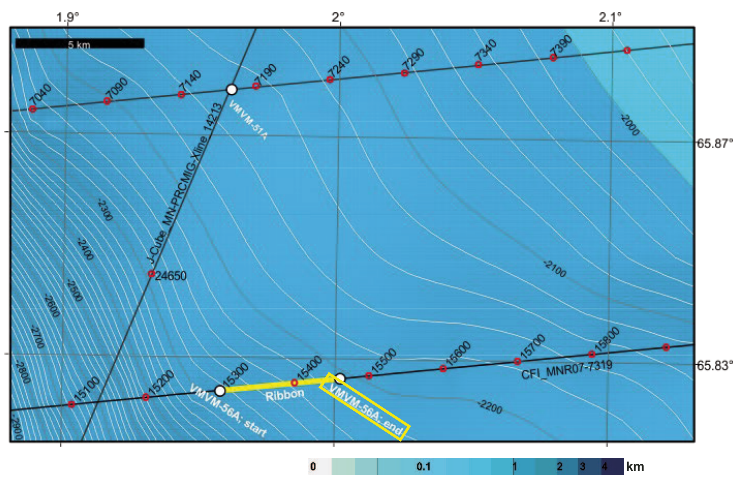

Figure AF17. Track map and seismic profiles, primary Proposed Site VMVM-61A. SP = shotpoint. SSDB = Site Survey Data Bank.

Site Figure for VMVM-61A | Primary

Coordinates: 67.30670° N, 3.73746° E (WGS84)
Water depth: 1200 m
Penetration: 300 m

Data

Remarks: Two 3D seismic volumes are available in the area: pre stack time migration (PSTM) and pre-stack depth migration (PSDM).

Site location:
CVX1101-PSTM-Inline_1852 (SP-3267) // CVX1101-PSTM-Xline_5057 (SP-1062)

Data files in SSDB: Seismic SEG-Y profiles extracted from 3D cube, velocity data.

Additional data: Velocity cube, gravity grids, magnetic grids and seafloor sampling report (VS16).

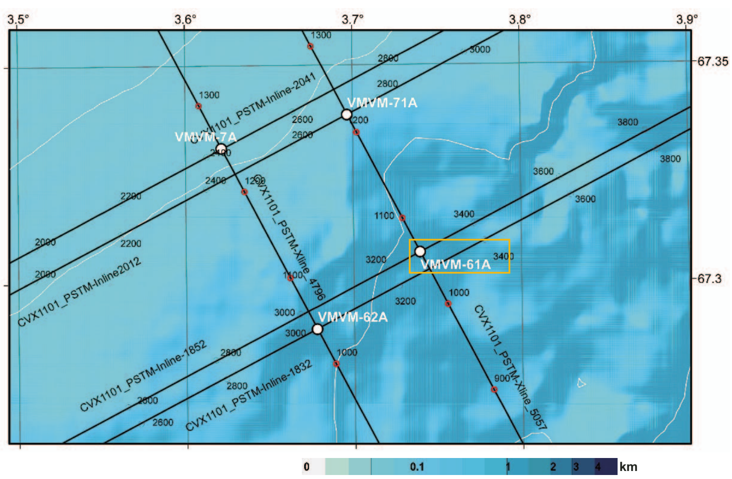

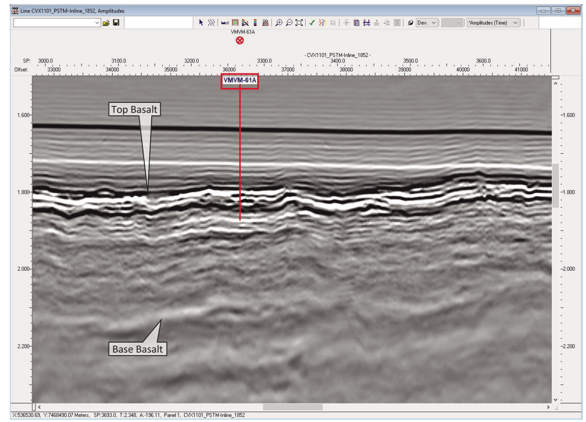

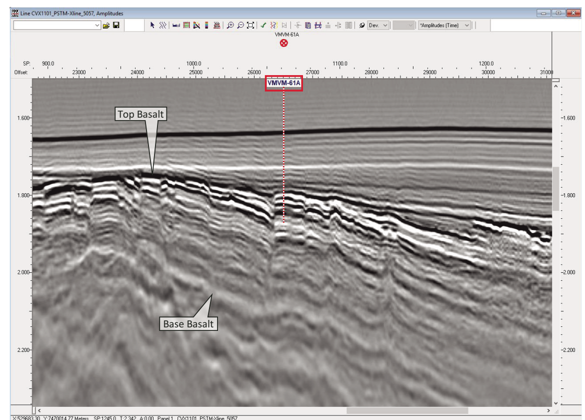

Figure AF18. Track map and seismic profiles, alternate Proposed Site VMVM-62A. SP = shotpoint. SSDB = Site Survey Data Bank.

Site Figure for VMVM-62A | Alternate

Coordinates: 67.28910° N, 3.67576° E (WGS84)
Water depth: 1198 m
Penetration: 300 m

Data

Remarks: Two 3D seismic volumes are available in the area: pre stack time migration (PSTM) and pre-stack depth migration (PSDM).

Site location:
CVX1101-PSTM-Inline_1832 (SP-3006) // CVX1101-PSTM-Xline_4796 (SP-1042)

Data files in SSDB: Seismic SEG-Y profiles extracted from 3D cube, velocity data.

Additional data: Velocity cube, gravity grids, magnetic grids and seafloor sampling report (VS16).

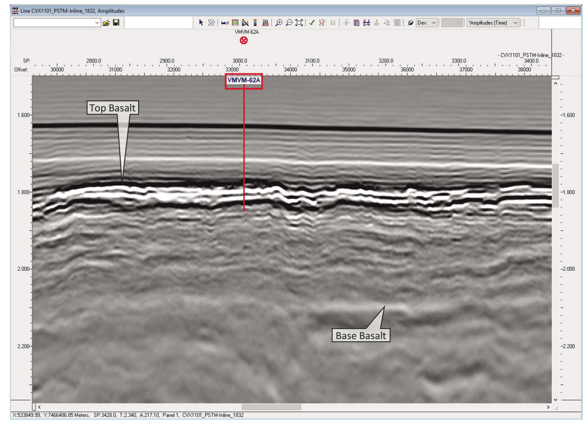

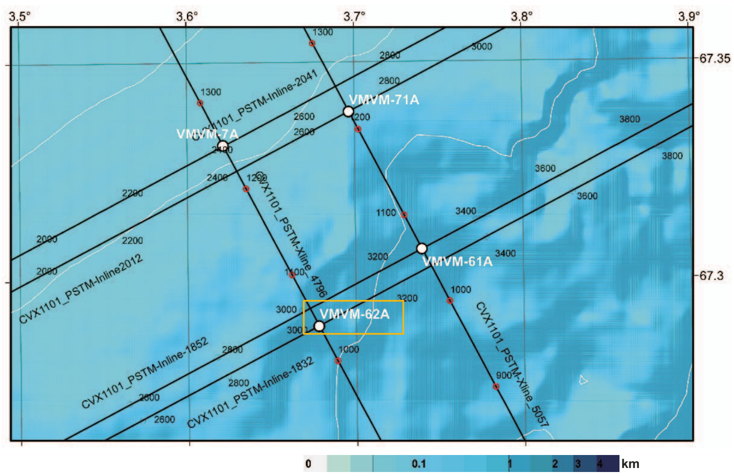

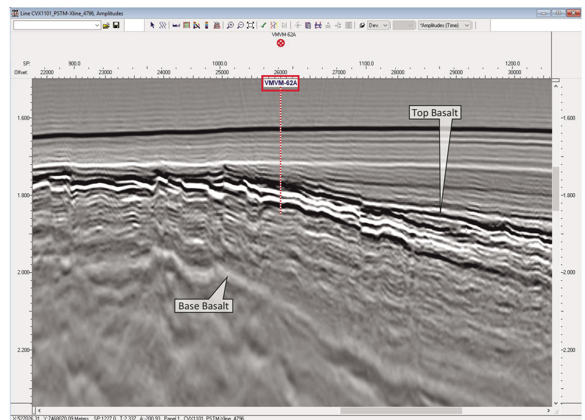

Figure AF19. Track map and seismic profiles, primary Proposed Site VMVM-07A. SP = shotpoint. SSDB = Site Survey Data Bank. SDR = seaward-dipping reflector.

Site Figure for VMVM-7A | Primary

Coordinates: 67.33080° N, 3.61935° E (WGS84)
Water depth: 1206 m
Penetration: 400 m

Data

Remarks: Two 3D seismic volumes are available in the area: pre stack time migration (PSTM) and pre-stack depth migration (PSDM).

Site location:
CVX1101-PSTM-Inline_2041 (SP-2436) // CVX1101-PSTM-Xline_4796 (SP-1251)

Data files in SSDB: Seismic SEG-Y profiles extracted from 3D cube, velocity data.

Additional data: Velocity cube, gravity grids, magnetic grids and seafloor sampling report (VS16).

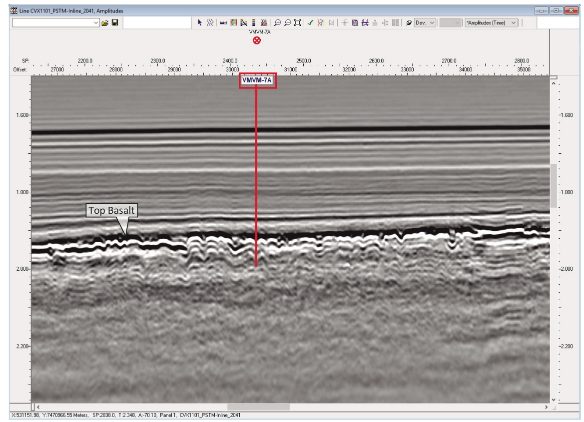

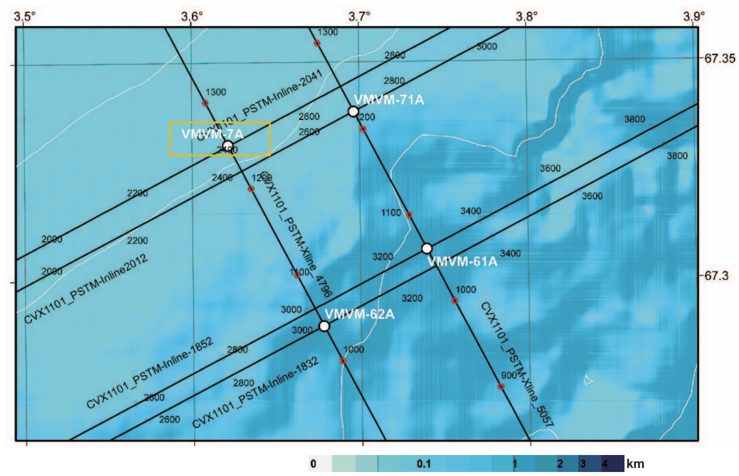

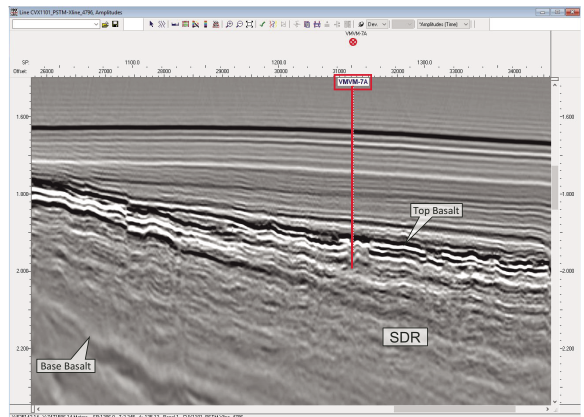

Figure AF20. Track map and seismic profiles, alternate Proposed Site VMVM-71A. SP = shotpoint. SSDB = Site Survey Data Bank. SDR = seaward-dipping reflector.

Site Figure for VMVM-71A | Alternate

Coordinates: 67.33840° N, 3.69456° E (WGS84)
Water depth: 1200 m
Penetration: 400 m

Data
Remarks: Two 3D seismic volumes are available in the area: pre stack time migration (PSTM) and pre-stack depth migration (PSDM).

Site location:
CVX1101-PSTM-Inline_2012 (SP-3267) // CVX1101-PSTM-Xline_5057 (SP-1222)

Data files in SSDB: Seismic SEG-Y profiles extracted from 3D cube, velocity data.

Additional data: Velocity cube, gravity grids, magnetic grids and seafloor sampling report (VS16).

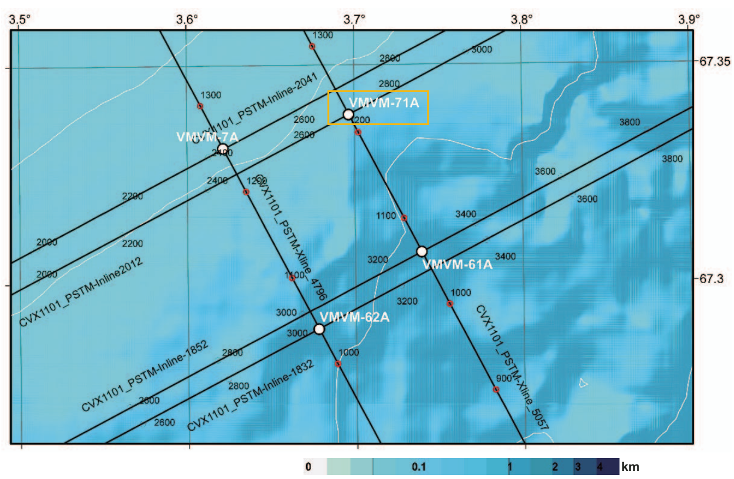

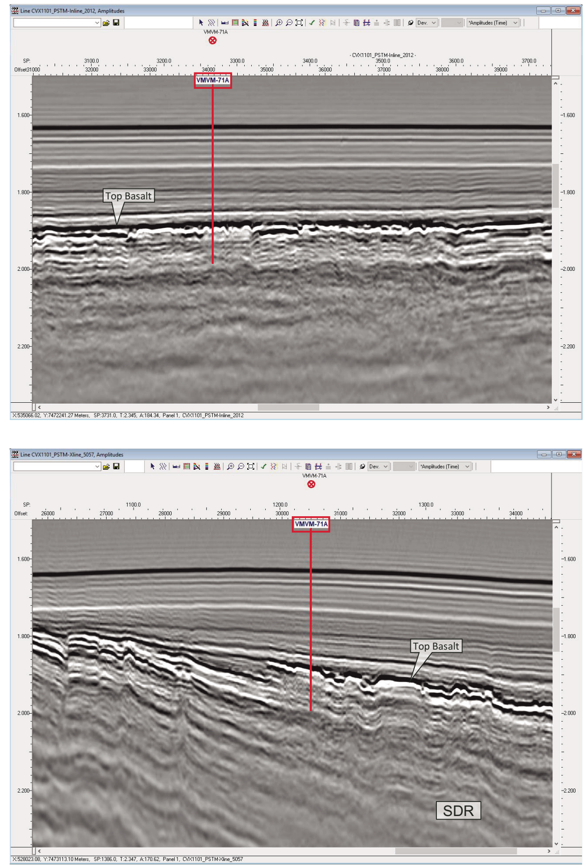

Figure AF21. Track map and seismic profile, primary Proposed Site VMVM-80A. SP = shotpoint. SSDB = Site Survey Data Bank.

Site Figure for VMVM-80A | Primary

Coordinates: 68.60020° N, 4.64057° E (WGS84)
Water depth: 2864 m
Penetration: 310 m

Data

Remarks: 2D seismic data is available in the area.

Site location:
HV96-7 (SP-4728)

Data files in SSDB: Seismic SEG-Y profiles and velocity data.

Additional data: DSDP boreholes 338, 342, 343.

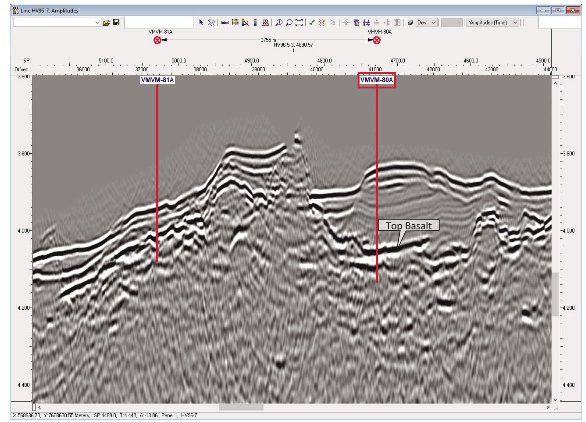

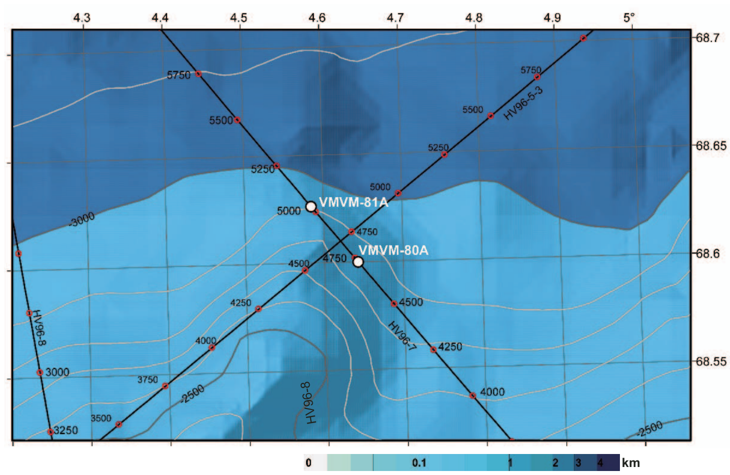

Figure AF22. Track map and seismic profile, alternate Proposed Site VMVM-81A. SP = shotpoint. SSDB = Site Survey Data Bank.

Site Figure for VMVM-81A | Alternate

Coordinates: 68.62640° N, 4.58257° E (WGS84)
Water depth: 2913 m
Penetration: 200 m

Data
Remarks: 2D seismic data is available in the area.

Site location:
HV96-7 (SP-5030)

Data files in SSDB: Seismic SEG-Y profiles and velocity data.

Additional data: DSDP boreholes 338, 342, 343.

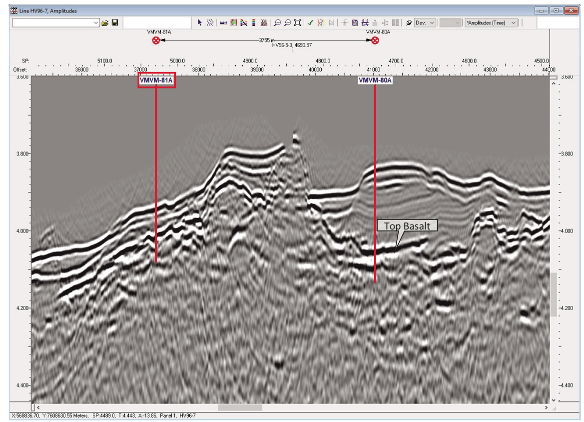

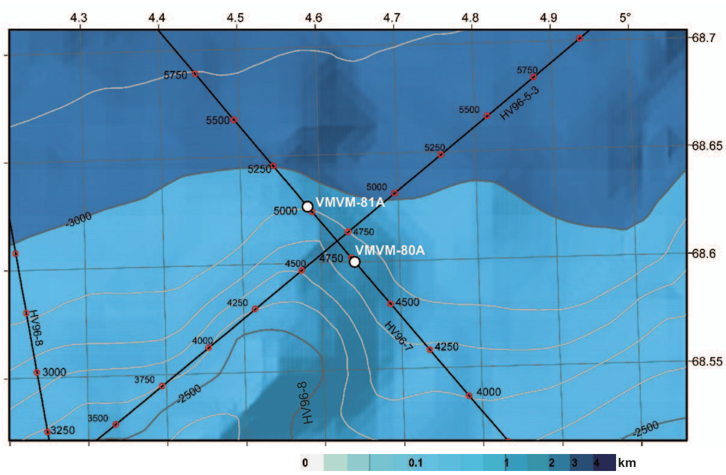

Figure AF23. Track map and seismic profile, primary Proposed Site VMVM-09A. SP = shotpoint. SSDB = Site Survey Data Bank.

Site Figure for VMVM-9A | Primary

Coordinates: 68.76040° N, 5.79491° E (WGS84)
Water depth: 3156 m
Penetration: 550 m

Data
Remarks: 2D seismic data is available in the area.

Site location:
HV96-6 (SP-2355)

Data files in SSDB: Seismic SEG-Y profiles and velocity data.

Additional data: DSDP boreholes 338, 342, 343.

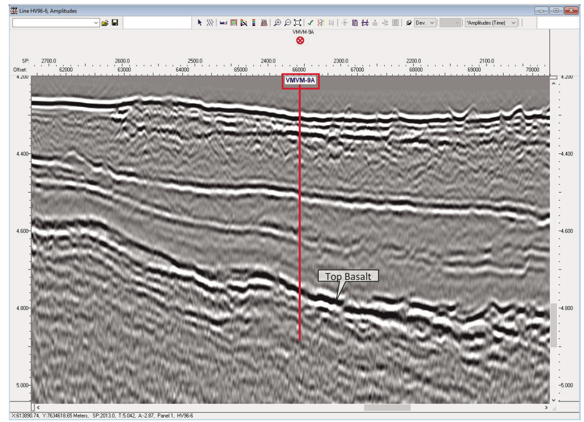

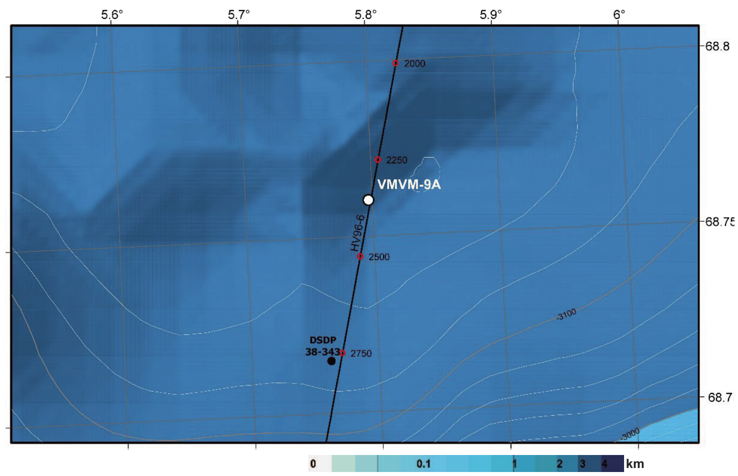

Figure AF24. Track map and seismic profiles, alternate Proposed Site VMVM-10B. SP = shotpoint. SSDB = Site Survey Data Bank.

Site Figure for VMVM-10B | Alternate

Coordinates: 68.83040° N, 4.12833° E (WGS84)
Water depth: 3237 m
Penetration: 750 m

Data
Remarks: 2D seismic data is available in the area.

Site location:
HV96-7 (SP-7370) // HV96-8 (SP-495)

Data files in SSDB: Seismic SEG-Y profiles and velocity data.

Additional data: DSDP boreholes 338, 342, 343.